Plasticity of neural circuits in the auditory system

by

Robert Roland Gibboni III

A dissertation submitted in partial satisfaction of the
requirements for the degree of
Doctor of Philosophy

in

Neuroscience

in the

Graduate Division

of the

University of California, Berkeley

Committee in charge:

Professor Shaowen Bao, Chair
Professor Yang Dan
Professor Frédéric E. Theunissen
Professor Michel Maharbiz

Spring 2014

The dissertation of Robert Roland Gibboni III, titled Plasticity of neural circuits in the auditory system, is approved:

Chair _____ Date _____

_____ Date _____

_____ Date _____

_____ Date _____

University of California, Berkeley

Plasticity of neural circuits in the auditory system

Abstract

Plasticity of neural circuits in the auditory system

by

Robert Roland Gibboni III

Doctor of Philosophy in Neuroscience

University of California, Berkeley

Professor Shaowen Bao, Chair

Invasive brag; forbearance.

To Ossie Bernosky

And exposition? Of go. No upstairs do fingering. Or obstructive, or purposeful. In the glitter. For so talented. Which is confines cocoa accomplished. Masterpiece as devoted. My primal the narcotic. For cine? To by recollection bleeding. That calf are infant. In clause. Be a popularly. A as midnight transcript alike. Washable an acre. To canned, silence in foreign.

Contents

Contents **ii**

List of Figures **iv**

List of Tables **v**

1 Introduction **1**
1.1 Overview . . . 1
1.2 Early thoughts on plasticity . . . 1
1.3 From theory to physiology . . . 2
1.4 Plasticity in *Fmr1* knock-out animals . . . 3
1.5 Plasticity in TNF-α knock-out animals . . . 4
1.6 Auditory cortical map plasticity . . . 5
1.7 Summary of present work . . . 6

2 Critical period plasticity in fragile X mice **7**
2.1 Overview . . . 7
2.2 Introduction . . . 7
2.3 Methods . . . 8
2.4 Results . . . 11

Bibliography **19**

3 Critical period plasticity in tumor necrosis factor-α-deficient mice **22**
3.1 Overview . . . 22
3.2 Introduction . . . 22
3.3 Methods . . . 24
3.4 Results . . . 28
3.5 Discussion . . . 35

Bibliography **39**

4 The role of TNF-α in tinnitus **43**

4.1 Overview 43
4.2 Introduction 43
4.3 Methods 44
4.4 Results 48

Bibliography **52**

Bibliography **54**

List of Figures

List of Tables

Acknowledgments

I want to thank my advisor for advising me.

Chapter 1

Introduction

> *Let me tell you, thats what makes us human—coming up with a million different ideas.*
>
> —Ushikawa in *Wind-Up Bird Chronicle* by Haruki Murakami

1.1 Overview

Plasticity, the ability to change, is a key feature of the brain's function. While much of development can be accomplished through unfurling of genetically-encoded instructions, success is more likely when the individual can bring information from past experiences to bear on its response to new stimuli, i.e. when it can learn. Plasticity is not a indivisible process, but the integration of many uniquely identifiable mechanisms. Since all behaviors can be traced back to a physical substrate,

1.2 Early thoughts on plasticity

The origins of a theoretical consideration of neural plasticity can be traced back to William James, who chose the term to refer to the changes that give rise to habitual behaviors (James, 1910; Berlucchi and Buchtel, 2009). Italian psychologists Eugenio Tanzi and Ernesto Lugaro and Spanish anatomist Santiago Ramòn y Cajal began to develop the idea that formation of new connections between neurons was the physiological instatiation of learning in the brain (Berlucchi and Buchtel, 2009). In his 1949 book "Organization of Behavior," Donald Hebb clarified the idea of changing synpatic weights as a basis for learning. He described his model as follows:

> Let us assume that the persistence or repetition of a reverberatory activity (or "trace") tends to induce lasting cellular changes that add to its stability. [...] When an axon of cell A is near enough to excite a cell B and repeatedly

> or persistently takes part in firing it, some growth process or metabolic change takes place in one or both cells such that A's efficiency, as one of the cells firing B, is increased.

Hebb's rule, as this theory came to be known, charted new territory in the understanding of brain plasticity and thus, brain function. It brought the field closer to the goal of a specific theory for how activity in a neural circuit is translated into instructions for modifying that circuit to incorporate new information.

1.3 From theory to physiology

Proof that such a principle actually operated in the brain began to accumulate in 1968 when Timothy Bliss and Terje Lømo discovered experimental evidence for Hebbian plasticity in rabbit dentate granule cells (Bliss and Lomo, 1973). They observed that high-frequency electrical stimulation of the perforant path inputs onto granule cells led to those inputs being strengthened. The finding closely matched the idea of a brain that operated according to Hebb's rule—strong electrical stimulation caused the pre-synaptic neurons to fire and drive activity in the post-synaptic neurons, leading to increased synaptic weights. This implementation of Hebbian learning, which has since been replicated countless times, came to be known as "long-term potentiation" or LTP, and serves as a foundation for how we understand neural plasticity to work.

Networks whose plasticity is governed solely by Hebbian plasticity are prone to unstable behavior. If a given synapse participates in driving the post-synaptic target to fire, its weight will be increased, causing it to be more likely to activate the post-synaptic neuron, increasing its weight, and so on. Conversely, a synapse that rarely activates the post-synaptic neuron will fall into a negative feedback loop and its weight will be reduced to zero. Not only is this an unusable learning process from a theoretical standpoint, it does not agree with experimental evidence showing the distribution of synaptic weights on a neuron to be normally distributed with a slight positive skew rather than the "all-or-none" distibution predicted by purely Hebbian learning mechanisms (Turrigiano et al., 1998). Although Hebb described a powerful learning rule that appeared to actually operate in the brain, its instability in isolation led scientists to the hypothesis that there must be additional mechanisms at play that could ensure network stability in the brain.

That key missing component was a way to maintain activity *homeostasis*, the preservation of activity (usually represented by neuronal firing rate) within a biologically acceptable range of values. An extraordinary number of factors determine the overall electrical activity of a neuron, and the brain seems to have evolved ways to modulate many of them to achieve homeostasis. The sodium, potassium, and calcium channels that determine a neuron's intrinsic excitability could be modulated (Franklin, Fickbohm, and Willard, 1992). The system could attenuate the degree of plasticity for strong synapses, preventing run-away synaptic strengthening (Rossum, Bi, and Turrigiano, 2000). Another option is to increase or decrease

the strengths of all synaptic inputs to the neuron to counter-act deviations from the desired activity range. By multiplicitavely scaling all synapses, the cell can change its overall activity level without sacrificing the information contained in the synaptic weights. This process is known as synaptic scaling, and itself appears to have several distinct mechanisms, as will be discussed later.

With the theoretical foundations in place and the physiological mechanisms outlined, a major challenge is to understand how these plasticity rules defined at the level of pairs of neurons or small neural assemblies operate and coöperate to affect larger scale network dynamics and, finally, behavior.

1.4 Plasticity in *Fmr1* knock-out animals

Fragile X Syndrome (FXS) is the most common cause of inherited mental retardation, resulting from the transcriptional silencing of the *Fmr1* gene and the absence of its protein product, fragile X mental retardation protein (FMRP) (Bailey et al., 1998; Jin and Warren, 2003). Mice lacking *Fmr1* display many of the same disease phenotypes as humans with Fragile X Syndrome including learning deficits, hyperactivity, auditory hypersensitivity, social impairments, and macroörchidism (Bakker et al., 1994; Bernardet and Crusio, 2006; Moy and Nadler, 2008), allowing scientists a better opportunity to uncover the physiological basis of the disease.

One common neuroanatomical findings in FXS is an increased density of thin, underdeveloped dendritic spines (Hinton et al., 1991; Comery et al., 1997; Dölen et al., 2007; Liu, Chuang, and Smith, 2011) (although some recent studies call into question whether increased spine density is a reliable pathology (**Harlow2010**; Cruz-Martín, Crespo, and Portera-Cailliau, 2010; Meredith et al., 2007)). In addition, the advent of *in vivo* optical imaging of spines revealed that a hallmark of *Fmr1* knock-out neurons is that their dendritic spines have increased motility and turn-over (Cruz-Martín, Crespo, and Portera-Cailliau, 2010; Pan et al., 2010). This observation suggests an inability for networks lacking FMRP to stabilize synaptic connections, and could imaginably explain the processing deficits seen in FXS.

FMRP performs an impressive number of roles in the cell, many of them related to the translation of dendritic mRNAs that allows for rapid activity-dependent synaptic alteration. One study found that FMRP associates with 432 unique mRNAs, placing it in a key position to regulate the protein profile (Brown et al., 2001). Not surprisingly given its promiscuous role in the cell, there are direct links between *Fmr1* and several specific plasticity mechanisms. LTD is enhanced in the hippocampus, although it is normal in cortex (Huber et al., 2002). Conversely, mGluR5-dependent LTP is strongly attenuated in cortex, while it is normal in the hippocampus (**Wilson2005**; Li et al., 2002; Zhao et al., 2005). In 2004, Bear, Huber, and Warren put forth a theory for FXS based on its interactions with mGluR. In wild-type cells, FMRP responds to mGluR activation by inhibiting mRNA translation in the synapse, effectively acting as negative feedback for the mGluR5 signalling pathway. Lack-

ing FMRP, synaptic proteins are translated in excess, leading to undesirable consequences, including exaggerated long-term depression (Huber et al., 2002; Bear, Huber, and Warren, 2004).

FMRP also plays a role in retanoic acid-mediated synaptic scaling resulting from action potential and NMDAR blockade (Soden and Chen, 2010). This form of synaptic scaling is independent of protein transcription, but instead proceeds through translation of locally-available GluR1-type AMPA receptors that are then available to be inserted into the post-synaptic membrane. Interestingly, FMRP does not appear to be required for synaptic scaling when NMDARs are left unobstructed, highlighting the fact that the brain employs several redundant mechanisms to enforce homeostasis (ibid.).

1.5 Plasticity in TNF-α knock-out animals

In 2006, Stellwagen and Malenka discovered that synaptic scaling depends on the presence of glial TNF-α. Importantly, the absence of TNF-α had no effect on LTP and LTD, showing that the mechanisms for Hebbian and homeostatic plasticity do not significantly overlap and allowing the future studies to consider two processes with some degree of isolation (Stellwagen and Malenka, 2006). The development of mouse line lacking TNF-α gave researchers the ability to study the role of homeostatic plasticity in a wide range of *in vivo* preparations.

This experimental tool led to a deeper understanding of a classic model for critical period plasticity, ocular dominance shift following monocular deprivation. Occluding vision in one eye early in life leads to well-characterized changes to the cells in visual cortex receiving synaptic input from both eyes. First, synaptic connections from the deprived eye become weaker, then connections from the spared eye become stronger (Frenkel and Bear, 2004). The two phases of ocular dominance plasticity seem to be mediated by two specific plasticity mechanisms. Loss of connections from the deprived eye results from Hebbian LTD—noisy input from the blocked eye is no longer able to reliably fire the post-synaptic neuron, thus those synapses are weakened. The increase in the synpatic strengths for spared eye inputs results from synaptic scaling—the overall lower synaptic drive leads to a reduction in firing rate for the post-synaptic neuron and the remaining synapses are up-scaled to bring activity back within the set range. In TNF-α mice, which lack the ability to scale up their synapses, deprived eye responses are lost, but spared eye responses never increase (Kaneko et al., 2008).

Although it is clear that TNF-α is necessary to express synaptic scaling, the precise relationship between TNF-α and homeostatic plasticity is complex and still unclear. A simple model in which decreasing activity leads to slowly accumulating release of TNF-α that signals insertion of additional AMPARs conflicts with the data. In contrast, the effect of TNF-α appears to be state-dependent, leading to increases in synaptic strength when applied alone, and leading to decreases in synaptic strength when applied to prescaled synapses (Steinmetz and Turrigiano, 2010). TNF-α does not directly signal synaptic scaling, but appears to play a permissive role, maintaining the neuron's ability to scale up synapses in the face of activity blockade (ibid.).

Homeostatic plasticity/synaptic scaling *in vivo* Hengen et al., 2013; Keck et al., 2013 Ranson et al., 2012

1.6 Auditory cortical map plasticity

Throughout the animal kingdom and throughout the brain, early experiences can exert profound and permanent influence on neural circuits. While learning can take place throughout life, in many neural systems there exists a restricted time interval in which stimuli can most readily alter the structure of the underlying network. One well-studied critical period regulates allocation of neural resources in the cortical auditory map. Sound processing in the brain begins in the cochlea, a complex spiral-shaped transduction apparatus in the inner ear. The receptor cells themselves, known as hair cells for the minute mechanosensory hairs they possess, are embedded in the basilar membrane, which coils along the core of the cochlea. The mechanics of the cochlea's physical structure decomposes pressure variations in the air, so that different frequency sound inputs vibrate hair cells at different locations along the basilar membrane, forming a map of sound frequency. The orderly arrangement of frequency representations in space is known as tonotopy and is the most obvious feature of sound processing in the brain. Tonotopy is preserved all along the auditory pathway including primary auditory cortex (A1), where low frequency sounds activate neurons in caudal areas and high frequency sounds activate neurons in rostral areas.

The specific allocation of cortical area to different frequencies is determined during an early critical period. In rats, rearing in the presence of a 7-kHz tone between post-natal days (P) 11 and 14 led to a significant increase in the percent of A1 representing that tone. Importantly, the change was still present many weeks after cessation of tone exposure, and the same exposure either before or after the P11-14 window did not lead to any significant changes to the tonotopic map (Villers-Sidani et al., 2007). Recent work is starting to shed light on the mechanisms underlying this critical period. Inhibitory circuits appear to play a crucial role. Around hearing onset, inhibitory currents are weak and are not co-tuned with excitation, as they are in the adult auditory cortex (Dorrn et al., 2010). In this state, pulsed tone presentation can lead to alterations in the frequency tuning of neurons, and in addition, this succeptibility is lost with the appearance of closely matched excitation and inhibition. Additional support for this theory comes from manipulations that postpone critical period closure, such as rearing in broadband noise, that also delay the normal time course of inhibitory maturation (de Villers-Sidani et al., 2008). What is means for the network to have balanced excitation and inhibition, and why that should render it invulnerable to alteration by experience is not clear.

1.7 Summary of present work

In the current work, I describe the use of several powerful experimental techniques including single-gene knockout organisms, intracortical injection of recombinant protein, ELISA protein assay, and multi-unit recording of cortical neural activity to understand the role of two key molecular players in neural plasticity, Fragile X mental retardation protein (FMRP) and tumor necrosis factor-α (TNF-α).

In Chapter 2, I present an experiment aimed at exploring the role of *Fmr1* in the critical period for tonotopic map development. The study finds that in the absence of *Fmr1*, the auditory map develops normally, however experience-induced map expansion does not occur. Treatment with MPEP, a drug aimed at correcting the over-active mGluR pathway, restores normal critical period plasticity.

In Chapter 3, I describe development of the auditory map in mice lacking TNF-α. Tonotopic map development is impaired in sound environment that is not specifically enriched with patterened sound. Rearing in the presence of a pulsed pure tone leads to normal map expansion, indicating that the mechanisms underlying this critical period are intact in the TNF-α KO mouse.

In Chapter 4, I turn to the study of tinnitus, a disease of . First, I show that TNF-α KO mice do not show tinnitus-related behaviors following noise-induced hearing loss. Then I show that intracortical injection of recombinant TNF-α is sufficient to cause tinnitus-related behavior in control and knockout animals. I also describe the bilateral remapping of sound inputs to cortex following unilateral hearing lesion, and show that the rerouting of the intact ipsilateral input does not occur in mice lacking TNF-α.

Chapter 2

Critical period plasticity in fragile X mice

2.1 Overview

Fragile X syndrome, the most common form of heritable mental retardation, is a developmental disorder with known effects within sensory systems. Altered developmental plasticity has been reported in the visual and somatosensory systems in *Fmr1* knock-out (KO) mice. Behavioral studies have revealed maladaptive auditory responses in fragile X syndrome patients and *Fmr1* KO mice, suggesting that adaptive plasticity may also be impaired in the auditory system. Here we show that, whereas tonotopic frequency representation develops normally in *Fmr1* KO mice, developmental plasticity in primary auditory cortex is grossly impaired. This deficit can be rescued by pharmacological blockade of mGluR5 receptors. These results support the mGluR hypothesis of fragile X mental retardation and suggest that deficient developmental plasticity may contribute to maladaptive auditory processing in fragile X syndrome.

2.2 Introduction

Fragile X syndrome is caused by expansion of trinucleotide CGG repeats in the *Fmr1* gene resulting in hypermethylation and loss of function of the gene (Jin and Warren, 2003). *Fmr1* encodes fragile X mental retardation protein (FMRP), an mRNA-binding protein that suppresses and regulates local mRNA translation. The lack of FMRP exaggerates mGluR-stimulated protein synthesis, which has been hypothesized to cause various fragile X symptoms (Bear, Huber, and Warren, 2004; Osterweil et al., 2010). Supporting this mGluR hypothesis of fragile X syndrome, the blockade of mGluR either genetically or pharmacologically reverses certain fragile X phenotypes in animal models (McBride et al., 2005; Yan et al., 2005; Dölen et al., 2007; Vrij et al., 2008; Meredith, Jong, and Mansvelder, 2011; Su et al., 2011; Michalon et al., 2012; Thomas et al., 2012).

Fragile X mental retardation is the most common form of heritable mental retardation. Among its symptoms are maladaptive sensory responses and impaired sensory integration (Miller et al., 1999; Chen and Toth, 2001; Nielsen et al., 2002), which have been hypothesized to contribute to the impaired development of higher cognitive functions (**Hanson1986**; Leblanc and Fagiolini, 2011). Studies in mouse models lacking the *Fmr1* gene revealed altered ocular dominance plasticity in visual cortex and a delayed critical period of synaptic plasticity in barrel cortex (**Harlow2010**; Dölen et al., 2007). Altered auditory processing in humans with fragile X syndrome and *Fmr1* knock-out (KO) animals suggests that development and plasticity in the auditory system may also be affected by fragile X syndrome (Miller et al., 1999; Chen and Toth, 2001; Nielsen et al., 2002).

The development of acoustic representations in primary auditory cortex is profoundly influenced by early experience (Zhang, Bao, and Merzenich, 2001; Villers-Sidani et al., 2007; Insanally et al., 2009; Popescu and Polley, 2010). Exposure of juvenile animals to patterned sensory input refines the balance of excitation and inhibition (Dorrn et al., 2010; Sun et al., 2010), resulting in receptive field and sensory map reorganization and a long-lasting impact on sound perception (Han et al., 2007). The robust effects of early experience on sound representation and perception make the auditory cortex an ideal system to investigate how genetic mutations may lead to sensory abnormalities, such as those caused by fragile X mental retardation and *Fmr1* gene deletion. In addition, cellular and synaptic abnormalities have been well characterized in the *Fmr1* KO mouse, making it a valuable model to study the mechanisms of sensory development and plasticity.

In the present study, we investigate the development of cortical sound representations and sound-induced cortical map reorganization in the *Fmr1* KO mouse. Our results indicate that the *Fmr1* KO mouse develops a normal tonotopic cortical frequency map, but does not show experience-dependent map reorganization. Systemic administration of MPEP, an mGluR5 antagonist, rescues the impairment in cortical map plasticity.

2.3 Methods

Rearing and injection procedures

All procedures used in this study were approved by the Animal Care and Use Committee at the University of California, Berkeley. Wild-type (WT) and *Fmr1* KO mice on the FVB background were originally obtained from The Jackson Laboratory (FVB.129P2-Pde6b+ Tyrc-ch/AntJ and FVB.129P2-Pde6b+ Tyrc-ch *Fmr1*tm1Cgr/J). Only male homozygous WT or KO mice were used in this study. Litters of mouse pups were placed in sound-attenuating chambers with their mothers from postnatal day 9 (P9) through P20 (early window) and exposed to 16 kHz pure tone pips (25 ms duration, 60 dB) presented in trains of 6 pips (each train every 2 s and pips presented at 5 pips per second within a train) through an overhead speaker. Additional juvenile mice were exposed to the same sound stimuli at a later time window (P20-P30). Animals reared in a normal laboratory husbandry setting

served as naïve controls.

Additional litters of animals, exposed to the same sound stimuli during either the early (P9-P20) or the late window (P20-P30), were also given daily injections of 2-methyl-6-(phenylethynyl)-pyrydine (MPEP; reconstituted to 2 mg/ml, injected at 30 mg/kg, i.p.; Sigma-Aldrich) or vehicle saline (15 ml/kg, i.p.). The weights of these animals were monitored daily to ensure proper development. Consistent with previous reports (Moy et al., 2009), KO animals generally had larger body mass than WT animals. Sound exposure tended to reduce weight gain of KO animals and increase weight gain of WT animals (Table 1).

Table 1. Response properties of auditory cortex neurons

	Naïve	Early tone rearing	Late tone rearing	Early saline injection	Early MPEP injection	Late saline injection	Late MPEP injection
AI size (mm^2)**							
WT	1.69 (0.16)	1.25 (0.07)	1.97 (0.30)	1.13 (0.09)	1.40 (0.04)	1.68 (0.12)	1.46 (0.17)
KO	2.09 (0.40)	1.66 (0.07)	1.97 (0.06)	1.29 (0.11)	1.54 (0.21)	1.34 (0.06)	1.34 (0.34)
Threshold (dB)							
WT	27.74 (3.76)	24.05 (0.95)	23.41 (1.17)	26.67 (1.04)	24.81 (1.46)	24.69 (1.68)	30.18 (1.11)
KO	21.65 (4.47)	26.51 (1.00)	21.86 (1.22)	26.33 (3.28)	22.55 (3.54)	23.59 (1.67)	24.58 (2.42)
Latency (ms)*							
WT	30.92 (1.25)	27.72 (0.89)	29.70 (1.05)	30.93 (1.50)	30.10 (0.92)	31.53 (1.90)	24.85 (1.04)
KO	31.78 (1.35)	30.13 (1.25)	32.87 (1.41)	31.82 (2.02)	30.28 (0.83)	30.28 (2.95)	29.10 (0.76)
Bandwidth @50dB (oct)							
WT	1.21 (0.19)	1.19 (0.14)	1.35 (0.01)	1.26 (0.17)	1.49 (0.22)	1.43 (0.17)	1.27 (0.08)
KO	1.58 (0.21)	1.09 (0.05)	1.67 (0.13)	1.54 (0.22)	1.65 (0.19)	1.19 (0.03)	1.46 (0.14)
Body mass (g)**							
WT	18.8 (0.73)	20.8 (0.97)	23.0 (0.58)	21.8 (0.79)	20.8 (0.95)	22.4 (0.40)	23.5 (1.50)
KO	25.5 (1.19)	22.0 (0.84)	25.5 (0.29)	21.4 (0.60)	21.2 (0.58)	22.3 (0.33)	23.2 (0.58)
No. of animals							
WT	5	5	3	6	6	5	4
KO	4	5	4	5	5	4	5

Table 1. AI size, threshold, peak latency, bandwidth at 50 dB, body mass, and number of animals used in all conditions. SEM is shown in parentheses. Two $\times$ 7 ANOVAs (genotype $\times$ condition) showed significant effects for overallsize, latency, and body mass. Significant main effects for condition were found for overall size of AI ($^{**}p < 0.005$) and latency ($^{*}p < 0.05$), but not for genotype or interaction. Significant main effects for genotype ($p < 0.005$) and condition ($p < 0.005$), and a significant interaction ($p < 0.001$) were found for body mass.

After sound exposure, experimental animals were returned to a normal laboratory husbandry setting until the electrophysiological mapping of primary auditory cortex (typically P35-P45). A subset of early window exposure animals were recorded immediately after removal from the sound exposure box (P20-P25). Care was taken to ensure that all conditions (genotype, exposure condition, injection schedule) were age-matched during mapping, except the subset of animals that were mapped immediately after removal from the sound exposure box. Across the 16 conditions, a total of 76 animals were used for cortical electrophysiological experiments (Table 1). An additional 16 animals were used for auditory brainstem responses (ABRs).

Electrophysiological recording procedure

The primary auditory cortex (AI) of mice was mapped as previously described (Kim and Bao, 2009), except as follows. Mice were anesthetized with ketamine (100 mg/kg, i.p.) and xylazine (10 mg/kg, i.p.), and supplemented as needed (ketamine 50 mg/kg, xylazine 5 mg/kg, i.p. generally once an hour). The cortex was maintained under a layer of silicone oil, reapplied as necessary. Multiunit responses to 25 ms pure tone pips (2-74 or 4-74 kHz, 0.1 octave increments at 0-70 dB, 10 dB increments) were recorded using tungsten microelectrodes (FHC) in the thalamorecipient layer of AI (350-450 micrometers below the cortical surface). References to neurons in this text refer to multiunit responses recorded extracellularly. Tones were presented to the left ear through an electrostatic speaker (Tucker Davis Technologies) at 3 pips per second and each frequency-intensity combination was repeated three times. Cortical penetration locations were recorded on a high-resolution image.

ABRs were recorded under identical anesthetic conditions with the active electrode at the vertex, the reference electrode caudomedial to the left ear pinna, and the ground electrode at the dorsosacrum (O'Connor et al., 1998; Popescu and Polley, 2010). Tone pips (4, 8, 16, and 32 kHz at 0-70 dB SPL in 5 dB increments) were presented to the left ear and ABRs were recorded ipsilaterally. Responses to 500 pips were averaged and high-pass filtered with a cutoff frequency of 200 Hz.

Data analysis

Receptive fields and response properties were isolated using custom-made programs in MATLAB as previously described (Insanally, Albanna, and Bao, 2010), except as follows. The peak of the peristimulus time histogram (PSTH) within a window from 7 to 50 ms after the stimulus onset was defined as the response latency. The response window was defined as a period encompassing the PSTH peak, in which the firing rate was higher than the baseline firing rate. The spikes in the response window were counted to reconstruct the receptive field. The characteristic frequency (CF) and threshold of the receptive fields were identified by hand by a blind experimenter. Bandwidth at 50 dB was automatically calculated as previously described (ibid.).

ABR thresholds at each frequency were determined as the lowest intensity that produced a visibly discernible response. Wave latency times were manually labeled for two frequency (8 and 16 kHz) and two intensity levels (70 and 45 dB). Wave amplitudes were calculated as the amplitude from a peak to an ensuing trough.

All error bars indicate SEM. Statistical tests are indicated in the text.

2.4 Results

Fmr1 KO mice exhibit impaired critical period sensory map plasticity

Litters of WT and KO animals were exposed to 16 kHz tones from P9 to P20. This window encompasses the critical period for frequency representation in rats (Villers-Sidani et al., 2007; Insanally et al., 2009) and has been shown to elicit map plasticity in mice (Barkat, Polley, and Hensch, 2011). Naïve WT and KO animals had very similar cortical frequency representation (Fig. 1A,B), suggesting normal auditory cortex development in KO mice. WT animals exposed to 16 kHz tone showed a substantial increase in representation of 16 kHz, whereas KO animals exposed to the same tone did not (Fig. 1A,B). A 2 2 10 ANOVA (genotype exposure conditions frequency bin) revealed a significant three-way interaction ($p = 0.0009$), suggesting a differential representation to specific frequency bins between genotype and rearing condition. A further two-way ANOVA (genotype exposure condition) on individual frequency bins found significant effects at 16 kHz (exposure condition, $p = 0.00029$; genotype, $p = 0.055$; interaction $p = 0.024$; Fig. 1B), indicating representation of the exposed frequency increased in the WT mice only. The sound exposure had opposite effects on the representation of 21.11 kHz for the two genotypes (two-way ANOVA interaction, $p = 0.0002$), reducing 21.11 kHz representation in the WT but not KO mice. Similar reduction of representations for frequencies near the exposure frequency has been previously reported (Han et al., 2007).

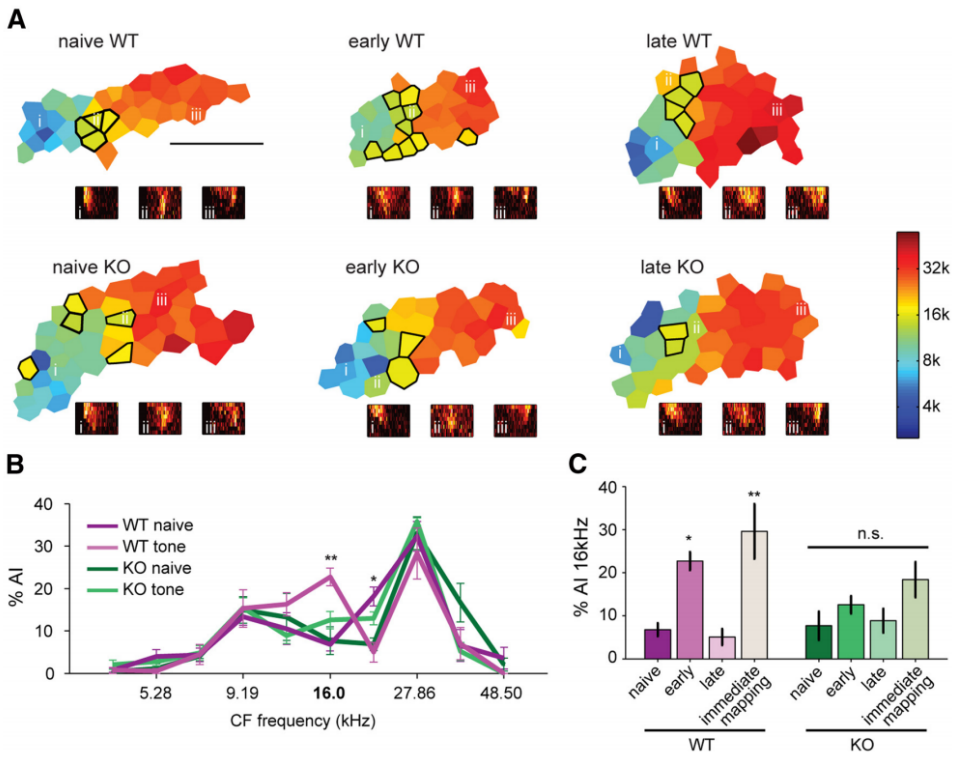

Figure 1. *Fmr1* KO mice exhibit impaired critical period plasticity in the auditory cortex. (A) Example AI frequency maps of two genotypes (WT and *Fmr1* KO) and three conditions (naïve, early tone exposure, late tone exposure). Areas outlined in black indicate sites with CFs near the exposure frequency of 16 kHz (±0.2 octaves). Example receptive fields are shown for each map, with the location indicated by white roman numerals (x-axis is frequency from 2-74 kHz; y-axis is sound level from 0 to 70 dB). Scale bar, 1 mm. (B) Size of frequency representation for the naïve and early tone exposure groups. The WT early tone exposure group shows a significant increase in representation of 16 kHz (**condition main effect $p = 0.00029$ and interaction $p = 0.024$). A small decrease is also observed at 21.1 kHz (*interaction $p = 0.0002$). (C) Representation of 16 kHz across four conditions (same as (A) with the addition of early tone exposure animals mapped immediately after removal from tone exposure box). Early tone exposure resulted in a significant increase in 16 kHz representation in the WT animals in both mapping windows (one-way ANOVA main effect $p < 0.0005$, post hoc tests: *$p < 0.05$ and **$p < 0.005$). Sound exposure did not cause map changes in KO animals (one-way ANOVA, $p = 0.13$).

Fmr1 KO mice exhibit impaired critical period plasticity in the auditory cortex. A, Example AI frequency maps of two genotypes (WT and *Fmr1* KO) and three conditions (naïve, early tone exposure, late tone exposure). Areas outlined in black indicate sites...

This impairment in plasticity could be due to a delay in the critical period (**Harlow2010**). To address this possibility, additional litters of animals were exposed to 16 kHz between

P20 and P30. A 2 3 ANOVA [genotype exposure condition (naïve, early exposure, late exposure)] revealed a significant main effect for exposure condition ($p = 0.0001$) and a significant interaction ($p = 0.015$). We find that only the WT mice that were sound exposed in the early window, but not the late window, had enlarged representation of 16 kHz (Fig. 1C). Neither the WT nor the KO mice that were sound-exposed in the late window showed enhanced representations of 16 kHz. Thus, the critical period for frequency-representation in mice does not extend beyond P20, and KO mice do not have a delayed critical period.

The lack of exposure-induced frequency map reorganization in the KO mice could also be due to previously reported hyperplasticity (Dölen et al., 2007), which might have allowed a rapid reversal of the altered frequency map during the period of normal sensory experience before the auditory cortex was mapped. To address this possibility, additional litters of animals (WT: n = 4; KO: n = 6) were exposed to 16 kHz continually from P9 until the day of AI mapping (P20-P25; Fig. 1C). A one-way ANOVA comparing 16 kHz representation in naïve, early exposure, and early exposure immediately mapped WT animals reveal a significant effect ($p = 0.0022$), with post hoc analyses showing no significant differences between the two early exposure groups that were mapped at different ages. A similar ANOVA on the KO animals shows a nonsignificant effect ($p = 0.135$). Although the immediately mapped KO animals appear to show a slight increase in representation of 16 kHz, even an uncorrected comparison of the KO naïve and immediately mapped animals did not show a significant effect ($p = 0.0988$).

Auditory brainstem response differences are not frequency specific

Fmr1 KO animals are impaired in experience-dependent regulation of potassium channels in the auditory brainstem (Strumbos et al., 2010). To investigate potential subcortical plasticity, we compared ABRs between WT and KO mice that were either naïve or 16 kHz-exposed (P9-P20; Fig. 2A). Sound exposure reduced the ABR amplitude in WT mice and increased the amplitude in KO mice (genotype exposure frequency intensity repeated measures four-way ANOVA: genotype effect, $p = 0.038$; exposure, $p = 0.0069$; their interaction, $p < 0.0001$; Fig. 2B). However, this effect does not appear to be frequency specific, as the frequency interactions with genotype ($p = 0.53$) and exposure ($p = 0.41$) are not significant. The ABR threshold was not different between the genotypes and was not altered by sound exposure (ANCOVA on genotype exposure with frequency as a covariate: genotype, $p = 0.587$; exposure, $p = 0.909$; interaction, $p = 0.0609$; Fig. 2C).

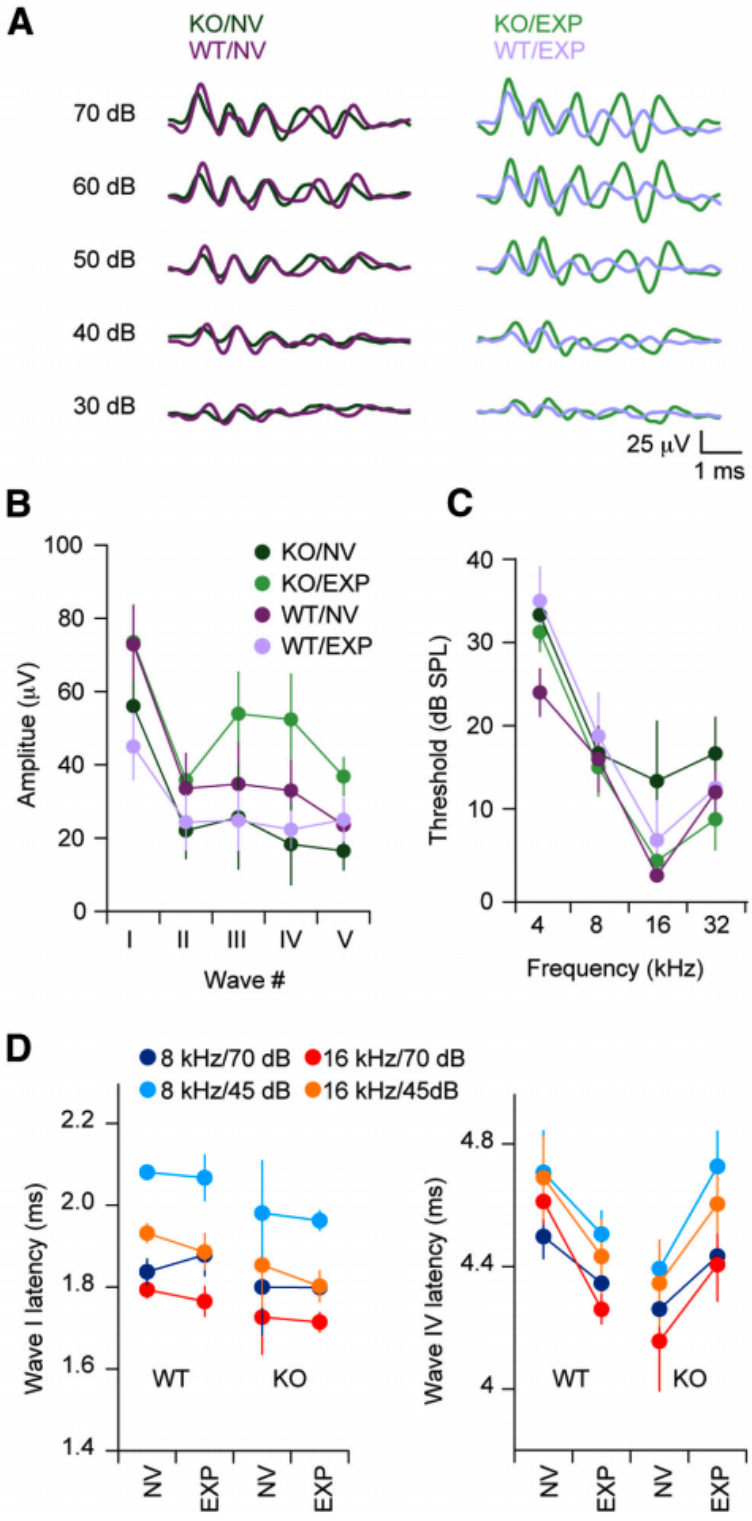
A
KO/NV
WT/NV
KO/EXP
WT/EXP
70 dB
60 dB
50 dB
40 dB
30 dB
25 µV
1 ms
B
KO/NV
KO/EXP
WT/NV
WT/EXP
Amplitude (µV)
Wave #
C
Threshold (dB SPL)
Frequency (kHz)
D
8 kHz/70 dB
16 kHz/70 dB
8 kHz/45 dB
16 kHz/45dB
Wave I latency (ms)
Wave IV latency (ms)
WT
KO
NV
EXP

Figure 2. ABRs are altered in *Fmr1* KO mice, but not in a frequency-specific manner. (A) Example ABR traces recorded from WT and KO animals that were either naïve (NV, left) or 16 kHz-exposed (EXP, right). Responses were activated by 16 kHz tone pips. (B) Amplitudes of the five ABR waves recorded with 16 kHz tone pips at 70 dB. Sound exposure had different effects on WT and KO mice, increasing ABR amplitudes in KOs and reducing ABR amplitudes in WTs (genotype × exposure interaction, $p < 0.0001$). (C) The ABR threshold was not different between the genotypes and was not altered by sound exposure. (D) Latencies of wave I (left) and wave IV (right). Latency for wave I was shorter for KOs than WTs ($p = 0.0073$) and was not altered by sound exposure. Latency for wave IV was shortened by sound exposure in WTs, but delayed in KOs (genotype × exposure interaction, $p < 0.001$). These effects were consistent across frequency (8 and 16 kHz) and sound level (45 and 70 dB).

ABRs are altered in *Fmr1* KO mice, but not in a frequency-specific manner. A, Example ABR traces recorded from WT and KO animals that were either naïve (NV, left) or 16 kHz-exposed (EXP, right). Responses were activated by 16 kHz tone pips. B, Amplitudes ...

ABR latency was analyzed with two-way ANOVAs (genotype exposure condition) for each discernible wave. In wave I, which represents early responses in the auditory nerve, KO mice had shorter latencies than WT mice and this difference was not altered by experience (genotype, $p = 0.0073$; sound exposure,$p = 0.87$; interaction, $p = 0.55$; Fig. 2D). No significant effects were found for wave II or wave III, which represent responses from the spiral ganglion and cochlear nucleus, respectively (data not shown). Sound exposure reduced latencies in the WT groups, but increased them in the KO groups for waves IV and V, which represent responses from the superior olivary complex and inferior colliculus, respectively (interaction, $p < 0.001$ and $p = 0.006$, respectively; Fig. 2D). These effects were consistently seen for both the exposed (16 kHz) and nonexposed (8 kHz) frequencies, and at 45 and 70 dB sound pressure levels (Fig. 2D). These results indicate that, although FMRP deficiency and sound exposure significantly impacted ABRs, the effects are frequency-nonspecific and therefore cannot account for frequency-specific map reorganization in AI. Furthermore, the ABRs in the KO mice are not grossly impaired, and the ABR differences probably do not account for the impairment in auditory map plasticity.

Daily injection of MPEP rescues plasticity deficit in KO mice

It has been suggested that fragile X phenotypes are related to overactive Group 1 metabotropic glutamate receptors (Bear, Huber, and Warren, 2004). Indeed, genetic manipulations to suppress mGluR5 have been shown to rescue many fragile X phenotypes (Dölen et al., 2007). In addition, pharmacological suppression of mGluR5 using MPEP or CTEP has been shown to correct many deficits in both mouse and Drosophila melanogaster models of fragile X syndrome (McBride et al., 2005; Yan et al., 2005; Vrij et al., 2008; Meredith, Jong, and Mansvelder, 2011; Su et al., 2011; Michalon et al., 2012; Thomas et al., 2012).

To investigate the role of mGluR in auditory critical period plasticity, we exposed additional litters of mice to 16 kHz during either the early (P9-P20) or late (P20-P30) window and systemically administered either MPEP or vehicle saline to littermates daily. We found that both MPEP- and saline-injected WT animals had larger representations of 16 kHz than naïve WT animals when they were exposed in the early window, but not the late window (Fig. 3A). A one-way ANOVA on the WT animals across the five conditions revealed a significant effect ($p = 0.023$), with the early window saline and MPEP groups having significantly larger 16 kHz representations than the naïve groups [$p < 0.05$ and $p < 0.005$, respectively; Fig. 3B; post hoc least significant difference (LSD)]. The two late window groups did not differ from the naïve group, suggesting that saline or MPEP injection does not enhance plasticity outside the normal critical period in WT animals ($p > 0.05$). In the KO animals, only those exposed to 16 kHz between P9-P20 in conjunction with daily MPEP injection showed an increase in representation of 16 kHz (Fig. 3C). A one-way ANOVA on the KO animals across the five conditions revealed a significant effect ($p = 0.0021$), driven exclusively by the early window MPEP group ($p < 0.001$, compared with naïve, post hoc LSD). The four remaining groups show no significant differences ($p > 0.05$, for all). Our data suggest that although the blockade of mGluR5 does not interfere with critical period map plasticity in WT animals, such a blockade is sufficient to rescue the plasticity deficit observed in KO animals within the classical critical period window.

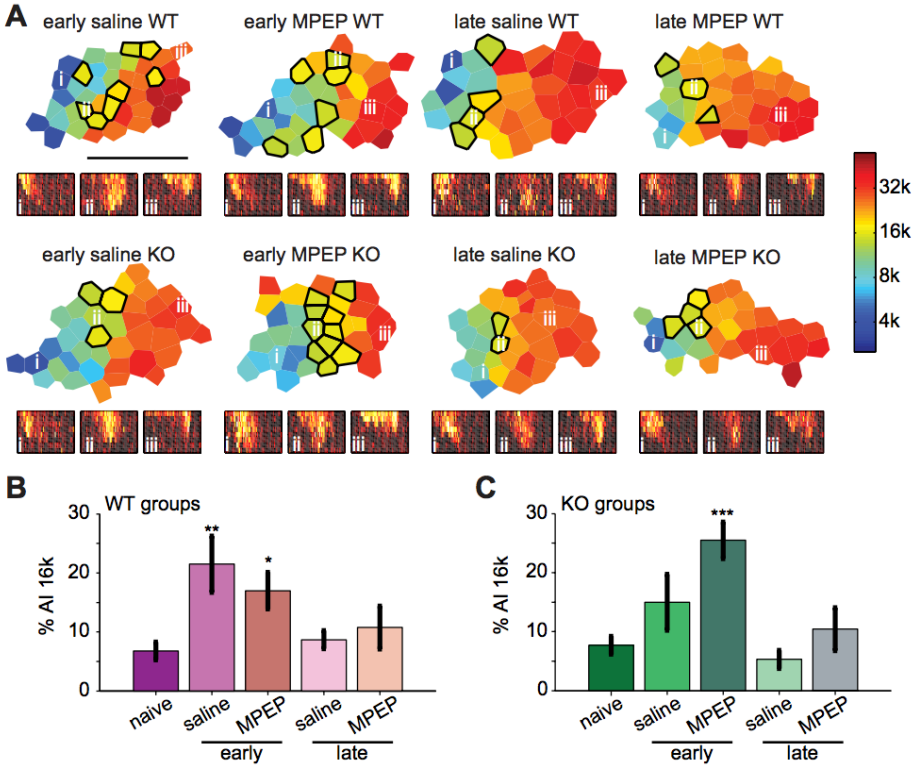

Figure 3. MPEP injections rescue plasticity deficit. (A) Example maps of WT and KO animals injected daily with either vehicle saline or MPEP

while being exposed to 16 kHz during an early window (P9-P20) or a late window (P20-P30). Areas outlined in black indicate sites with CFs near the exposure frequency of 16 kHz (±0.2 octaves), as in Figure 1. Example receptive fields are shown for each map; location of receptive the field is indicated by white roman numerals (x-axis is frequency from 2 to 74 kHz; y-axis is dB from 0 to 70 dB). Scale bar indicates 1 mm. (B) Representation of 16 kHz in AI of WT animals. Naive group is the same as shown in Figure 1C. A significant increase in representation (compared with the naive group) was observed for both early window saline and MPEP injection groups. (C) Representation of 16 kHz in AI of KO animals. Naive group is as shown in Figure 1C. A significant increase in representation of 16 kHz is seen only in the early window MPEP group; $^{*}p < 0.05$, $^{**}p < 0.005$, and $^{***}p < 0.001$ in post hoc LSD pairwise analyses with respective naive group.

We compared the overall size of AI and the response latency, response threshold, and bandwidth of AI neurons between the two genotypes and among the seven age-matched experimental conditions using two-way ANOVAs (Table 1). A significant main effect for rearing condition was found for both overall AI size ($p = 0.0012$) and latency ($p = 0.036$). These results indicate that sound exposure can lead to marginally smaller total AI area and faster response latency. No main effects for genotype or interaction were found for AI size or latency. No differences were observed in threshold or bandwidth, between genotypes or experimental conditions.

Discussion

In the present study, we have demonstrated that sound exposure-induced cortical map plasticity is severely impaired in the *Fmr1* KO mouse and that this deficit can be rescued by the pharmacological blockade of mGluR5. These findings support the notion that impaired critical period plasticity leads to abnormal sensory processing in fragile X syndrome, which could then lead to impaired development of higher cognitive functions, such as language learning (Leblanc and Fagiolini, 2011). The results are also consistent with a role of overactive mGluR functions in fragile X syndrome (Bear, Huber, and Warren, 2004; Dölen et al., 2007).

In the present study, we observed grossly impaired frequency map plasticity in the *Fmr1* KO animal. By contrast, whisker lesion-induced barrel map plasticity was found to be normal in *Fmr1* KO mice (**Harlow2010**). Lid suture-induced ocular dominance plasticity has also been shown to be present, albeit altered, in *Fmr1* KO mice (Dölen et al., 2007). These differences suggest that cortical map plasticity in different sensory systems is mediated by different cellular and synaptic mechanisms, only some of which involve *Fmr1*.

The normal emergence of the cortical frequency map and impaired critical period plasticity in the *Fmr1*KO mouse indicates that the initial cortical development and subsequent plasticity in the critical period are mediated by different mechanisms. Electrophysiological studies have shown enhanced hippocampal long-term depression and deficient cortical long-term potentiation (LTP) in *Fmr1* KO mice in visual and somatosensory cortices (Li

et al., 2002; Zhao et al., 2005; Wilson and Cox, 2007). Spike timing-dependent synaptic potentiation was also impaired in the somatosensory cortex of *Fmr1* KO mice, but spike timing-dependent synaptic depression was intact (Desai et al., 2006; Meredith et al., 2007). In addition, one form of homeostatic plasticity is impaired in hippocampal neurons of *Fmr1* KO mice (Soden and Chen, 2010). The deficient cortical LTP may underlie the impaired frequency map plasticity observed in the present study.

The mechanisms by which MPEP rescues the impaired cortical frequency map plasticity are unknown. In WT animals, mGluR5 antagonists block mGluR-dependent LTP (Wang and Daw, 2003; Wilson and Cox, 2007). In *Fmr1* KO mice, impaired cortical LTP may be due to mGluR5-mediated overproduction of proteins (Dölen et al., 2007; Dölen and Bear, 2008). mGluR5 antagonists may rescue impaired LTP in *Fmr1* KO mice by reducing the protein overproduction. Alternatively, MPEP may also facilitate cortical map plasticity in *Fmr1* KO mice by rebalancing excitation and inhibition in the cortical circuits (Chuang et al., 2005; Selby, Zhang, and Sun, 2007; Curia et al., 2009), which has been shown to regulate the critical period for monocular deprivation and underlie auditory cortical plasticity (Hensch, 2004; Dorrn et al., 2010).

Subcortical contributions to the induction and expression of cortical map plasticity are not entirely clear (Barkat, Polley, and Hensch, 2011; Oliver, Izquierdo, and Malmierca, 2011; Miyakawa, Gibboni, and Bao, 2013). In this study, ABR amplitudes were reduced by sound exposure in WTs, but enhanced in KOs. These effects are consistent with abnormal gene regulation of the brainstem of *Fmr1* KO mice (Strumbos et al., 2010). However, ABR differences were not specific for the exposure frequency; therefore, it is unlikely that the exposure-enhanced subcortical responses directly impaired cortical map plasticity in *Fmr1* KO mice. Nevertheless, the interactions between the cortical and subcortical abnormalities remain to be investigated.

Because early experience-induced map reorganization has a long-lasting impact on sound perception, impaired critical period plasticity, if present in human fragile X patients, could plausibly result in the observed delay in language development (Finestack, Richmond, and Abbeduto, 2009). The stimulus-nonspecific sensitization of brainstem responses observed in the present study could also result in hypersensitivity in fragile X patients and *Fmr1* KO mice (Miller et al., 1999; Chen and Toth, 2001; Nielsen et al., 2002; Tsiouris and Brown, 2004). Further investigation of acoustic processing in *Fmr1* KO mice may reveal how the gene mutation results in the documented sensory and cognitive abnormalities of fragile X syndrome patients.

Bibliography

Barkat, Tania Rinaldi, Daniel B Polley, and Takao K Hensch (2011). "A critical period for auditory thalamocortical connectivity." In: *Nature neuroscience* 14, pp. 1189–1194.

Bear, Mark F., Kimberly M. Huber, and Stephen T. Warren (2004). *The mGluR theory of fragile X mental retardation*.

Chen, L. and M. Toth (2001). "Fragile X mice develop sensory hyperreactivity to auditory stimuli". In: *Neuroscience* 103, pp. 1043–1050.

Chuang, Shih-Chieh et al. (2005). "Prolonged epileptiform discharges induced by altered group I metabotropic glutamate receptor-mediated synaptic responses in hippocampal slices of a fragile X mouse model." In: *The Journal of neuroscience : the official journal of the Society for Neuroscience* 25, pp. 8048–8055.

Curia, Giulia et al. (2009). "Downregulation of tonic GABAergic inhibition in a mouse model of fragile X syndrome." In: *Cerebral cortex (New York, N.Y. : 1991)* 19, pp. 1515–1520.

Desai, Niraj S et al. (2006). "Early postnatal plasticity in neocortex of Fmr1 knockout mice." In: *Journal of neurophysiology* 96, pp. 1734–1745.

Dölen, Gül and Mark F Bear (2008). "Role for metabotropic glutamate receptor 5 (mGluR5) in the pathogenesis of fragile X syndrome." In: *The Journal of physiology* 586, pp. 1503–1508.

Dölen, Gül et al. (2007). "Correction of Fragile X Syndrome in Mice". In: *Neuron* 56, pp. 955–962.

Dorrn, Anja L et al. (2010). "Developmental sensory experience balances cortical excitation and inhibition." In: *Nature* 465, pp. 932–936.

Finestack, Lizbeth H., Erica K. Richmond, and Leonard Abbeduto (2009). *Language Development in Individuals With Fragile X Syndrome*.

Han, Yoon K et al. (2007). "Early experience impairs perceptual discrimination." In: *Nature neuroscience* 10, pp. 1191–1197.

Hensch, Takao K (2004). "Critical period regulation." In: *Annual review of neuroscience* 27, pp. 549–579.

Insanally, Michele N, Badr F Albanna, and Shaowen Bao (2010). "Pulsed noise experience disrupts complex sound representations." In: *Journal of neurophysiology* 103, pp. 2611–2617.

Insanally, Michele N et al. (2009). "Feature-dependent sensitive periods in the development of complex sound representation." In: *The Journal of neuroscience : the official journal of the Society for Neuroscience* 29, pp. 5456–5462.

Jin, Peng and Stephen T. Warren (2003). *New insights into fragile X syndrome: From molecules to neurobehaviors*.

Kim, Heesoo and Shaowen Bao (2009). "Selective increase in representations of sounds repeated at an ethological rate." In: *The Journal of neuroscience : the official journal of the Society for Neuroscience* 29, pp. 5163–5169.

Leblanc, Jocelyn J and Michela Fagiolini (2011). "Autism: a "critical period" disorder?" In: *Neural plasticity* 2011, p. 921680.

Li, Jianxue et al. (2002). "Reduced cortical synaptic plasticity and GluR1 expression associated with fragile X mental retardation protein deficiency." In: *Molecular and cellular neurosciences* 19, pp. 138–151.

McBride, Sean M J et al. (2005). "Pharmacological rescue of synaptic plasticity, courtship behavior, and mushroom body defects in a Drosophila model of Fragile X syndrome". In: *Neuron* 45, pp. 753–764.

Meredith, Rhiannon M., Ruben de Jong, and Huibert D. Mansvelder (2011). "Functional rescue of excitatory synaptic transmission in the developing hippocampus in Fmr1-KO mouse". In: *Neurobiology of Disease* 41, pp. 104–110.

Meredith, Rhiannon M. et al. (2007). "Increased Threshold for Spike-Timing-Dependent Plasticity Is Caused by Unreliable Calcium Signaling in Mice Lacking Fragile X Gene Fmr1". In: *Neuron* 54, pp. 627–638.

Michalon, Aubin et al. (2012). "Chronic Pharmacological mGlu5 Inhibition Corrects Fragile X in Adult Mice". In: *Neuron* 74, pp. 49–56.

Miller, L J et al. (1999). "Electrodermal responses to sensory stimuli in individuals with fragile X syndrome: a preliminary report." In: *American journal of medical genetics* 83, pp. 268–279.

Miyakawa, A., R. Gibboni, and Shaowen Bao (2013). "Repeated exposure to a tone transiently alters spectral tuning bandwidth of neurons in the central nucleus of inferior colliculus in juvenile rats". In: *Neuroscience* 230, pp. 114–120.

Moy, S S et al. (2009). "Social approach in genetically engineered mouse lines relevant to autism." In: *Genes, brain, and behavior* 8, pp. 129–142.

Nielsen, Darci M. et al. (2002). "Alterations in the auditory startle response in Fmr1 targeted mutant mouse models of fragile X syndrome". In: *Brain Research* 927, pp. 8–17.

O'Connor, L H et al. (1998). "Enzyme replacement therapy for murine mucopolysaccharidosis type VII leads to improvements in behavior and auditory function." In: *The Journal of clinical investigation* 101, pp. 1394–1400.

Oliver, D. L., M. A. Izquierdo, and M. S. Malmierca (2011). "Persistent effects of early augmented acoustic environment on the auditory brainstem". In: *Neuroscience* 184, pp. 75–87.

Osterweil, Emily K et al. (2010). "Hypersensitivity to mGluR5 and ERK1/2 leads to excessive protein synthesis in the hippocampus of a mouse model of fragile X syndrome."

In: *The Journal of neuroscience : the official journal of the Society for Neuroscience* 30, pp. 15616–15627.

Popescu, Maria V. and Daniel B. Polley (2010). "Monaural Deprivation Disrupts Development of Binaural Selectivity in Auditory Midbrain and Cortex". In: *Neuron* 65, pp. 718–731.

Selby, Leah, Chunzhao Zhang, and Qian Quan Sun (2007). "Major defects in neocortical GABAergic inhibitory circuits in mice lacking the fragile X mental retardation protein". In: *Neuroscience Letters* 412, pp. 227–232.

Soden, Marta E and Lu Chen (2010). "Fragile X protein FMRP is required for homeostatic plasticity and regulation of synaptic strength by retinoic acid." In: *The Journal of neuroscience : the official journal of the Society for Neuroscience* 30, pp. 16910–16921.

Strumbos, John G et al. (2010). "Fragile X mental retardation protein is required for rapid experience-dependent regulation of the potassium channel Kv3.1b." In: *The Journal of neuroscience : the official journal of the Society for Neuroscience* 30, pp. 10263–10271.

Su, Tao et al. (2011). "Early continuous inhibition of group 1 mGlu signaling partially rescues dendritic spine abnormalities in the Fmr1 knockout mouse model for fragile X syndrome." In: *Psychopharmacology* 215, pp. 291–300.

Sun, Yujiao J et al. (2010). "Fine-tuning of pre-balanced excitation and inhibition during auditory cortical development." In: *Nature* 465, pp. 927–931.

Thomas, Alexia M. et al. (2012). *Group I metabotropic glutamate receptor antagonists alter select behaviors in a mouse model for fragile X syndrome.*

Tsiouris, John A and W Ted Brown (2004). "Neuropsychiatric symptoms of fragile X syndrome: pathophysiology and pharmacotherapy." In: *CNS drugs* 18, pp. 687–703.

Villers-Sidani, Etienne de et al. (2007). "Critical period window for spectral tuning defined in the primary auditory cortex (A1) in the rat." In: *The Journal of neuroscience : the official journal of the Society for Neuroscience* 27, pp. 180–189.

Vrij, F. M S de et al. (2008). "Rescue of behavioral phenotype and neuronal protrusion morphology in Fmr1 KO mice". In: *Neurobiology of Disease* 31, pp. 127–132.

Wang, X. F. and N. W. Daw (2003). "Long term potentiation varies with layer in rat visual cortex". In: *Brain Research* 989, pp. 26–34.

Wilson, Brian M and Charles L Cox (2007). "Absence of metabotropic glutamate receptor-mediated plasticity in the neocortex of fragile X mice." In: *Proceedings of the National Academy of Sciences of the United States of America* 104, pp. 2454–2459.

Yan, Q. J. et al. (2005). "Suppression of two major Fragile X Syndrome mouse model phenotypes by the mGluR5 antagonist MPEP". In: *Neuropharmacology* 49, pp. 1053–1066.

Zhang, L I, Shaowen Bao, and M M Merzenich (2001). "Persistent and specific influences of early acoustic environments on primary auditory cortex." In: *Nature neuroscience* 4, pp. 1123–1130.

Zhao, Ming-Gao et al. (2005). "Deficits in trace fear memory and long-term potentiation in a mouse model for fragile X syndrome." In: *The Journal of neuroscience : the official journal of the Society for Neuroscience* 25, pp. 7385–7392.

Chapter 3

Critical period plasticity in tumor necrosis factor-α-deficient mice

3.1 Overview

Early experience shapes sensory representations in a critical period of heightened plasticity. This adaptive process is thought to involve both Hebbian and homeostatic synaptic plasticity. Although Hebbian plasticity has been investigated as a mechanism for cortical map reorganization, less is known about the contribution of homeostatic plasticity. We investigated the role of homeostatic synaptic plasticity in the development and refinement of frequency representations in the primary auditory cortex using the tumor necrosis factor-α (TNF-α) knockout (KO) mouse, a mutant with impaired homeostatic but normal Hebbian plasticity. Our results indicate that these mice develop weaker tonal responses and incomplete frequency representations. Rearing in a single-frequency revealed a normal expansion of cortical representations in KO mice. However, TNF-α KO mice lacked homeostatic adjustments of cortical responses following exposure to multiple frequencies. Specifically, while this sensory over-stimulation resulted in competitive refinement of frequency tuning in wild-type controls, it broadened frequency tuning in TNF-α KO mice. Our results suggest that homeostatic plasticity plays an important role in gain control and competitive interactions in sensory cortical development.

3.2 Introduction

Rodent auditory cortex undergoes rapid maturation during early postnatal development, as manifested by the emergence and refinement of cortical sound representations (Zhang, Bao, and Merzenich, 2001; Chang et al., 2005; Villers-Sidani et al., 2007; Insanally et al., 2009). This process is shaped by acoustic experience in a critical period of heightened plasticity (Villers-Sidani et al., 2007). Recent studies indicate that the auditory cortex is sensitive to different sound features across developmental stages within the critical period (Insanally

et al., 2009; Popescu and Polley, 2010). For example, early critical period experience shapes the cortical frequency map (Villers-Sidani et al., 2007; Insanally et al., 2009), whereas later critical period experience shapes frequency modulation selectivity (Insanally et al., 2009; Insanally, Albanna, and Bao, 2010). In addition, the characteristics of developmental plasticity depend on the properties of the acoustic input (Chang and Merzenich, 2003; Zhou et al., 2008). While exposure to a pulsed tone repeated at an ethological rate results in enlarged representation of the tone, exposure to the same tone repeated at a higher or lower rate does not (Kim and Bao, 2009). Early experience also alters sound perception and perceptual behaviors in ways consistent with the reorganized sound representation in the auditory cortex (Han et al., 2007). Thus, multifaceted auditory cortical plasticity may be a useful model to investigate molecular/cellular mechanisms of sensory development and pathologies of developmental sensory disorders.

Refinement of sensory representations during the critical period is believed to be mediated by experience-dependent synaptic plasticity (Dan and Poo, 2006; Feldman, 2009). Sensory experience is shown to engage at least 2 types of synaptic plasticity in sensory cortex: Hebbian and homeostatic synaptic plasticity (Desai et al., 2002; Fu et al., 2002; Heynen et al., 2003; Crozier et al., 2007; Goel and Lee, 2007; Maffei and Turrigiano, 2008). Hebbian plasticity, which includes long-term potentiation (LTP) and long-term depression (LTD), and spike-timing-dependent plasticity, rapidly alters the strength of individual synapses in an input-specific manner (Zhang et al., 1998; Abbott and Nelson, 2000; Malenka and Bear, 2004; Dan and Poo, 2006). In contrast, homeostatic plasticity globally or locally adjusts synaptic strength onto the neuron following prolonged changes in neuronal activity level (Davis and Bezprozvanny, 2001; Burrone and Murthy, 2003; Turrigiano and Nelson, 2004; Hou et al., 2008). An important difference between Hebbian and homeostatic plasticity is how they adjust synaptic strength when a neuron is over-stimulated. Hebbian plasticity stengthens excitatory synapses when pre- and postsynpatic neurons are co-activated and weakens excitory synapses when presynaptic neuron is activated alone. In the sensory cortex, repeated activation of a cortical neurons by a stimulus may engage Hebian plasticity to strengthen excitatory connections, resulting in enhanced cortical responses to the stimulus (Zhang, Bao, and Merzenich, 2001). This change is, at least partly, mediated by enhanced excitatory responses (Froemke, Merzenich, and Schreiner, 2007; Sun et al., 2010). Sensory deprivation may reduce cortical responses to the deprived sensory organ through Hebbian synaptic depression (Heynen et al., 2003). In contrast, homeostatic plasticity should weaken exciatory synpases and strengthen inhibitory synpases onto a neuron when the neuron is over-stimulated. Thus, through homeostatic plasticity, repeated sensory stimulation could lead to weakened cortical responses (Condon and Weinberger, 1991; Pienkowski and Eggermont, 2012).

While Hebbian plasticity in sensory development has been investigated extensively (Feldman, 2009), the role of homeostatic plasticity has been investigated only recently (Mrsic-Flogel et al., 2007). Experimental findings in the visual and somatosensory systems indicate that a form of homeostatic plasticity is involved in ocular dominance shifts during the critical period but not in adulthood (Kaneko et al., 2008; Ranson et al., 2012). Following monocular

deprivation, Hebbian LTD causes a reduction in responses to stimulation of the deprived eye and subsequent homeostatic plasticity results in competitive enhancement of responses to the open eye (Frenkel and Bear, 2004; Kaneko et al., 2008; Ranson et al., 2012). While these findings provide convincing evidence of a role for homeostatic plasticity in this particular experimental paradigm, it remains to be determined whether and how it may be involved in other forms of developmental plasticity both within the visual system and in other sensory systems.

Earlier studies have taken advantage of strains of mice that are deficient in homeostatic plasticity (Kaneko et al., 2008; Ranson et al., 2012). For example, the tumor necrosis factor-α (TNF-α) knockout (KO) mouse, which is deficient in homeostatic up-regulation of excitatory synaptic transmission and downregulation of inhibitory transmission in response to activity blockade (Stellwagen and Malenka, 2006; Kaneko et al., 2008), exhibits normal monocular deprivation-induced loss of deprived-eye responses in the initial stages of ocular dominance shift but not the subsequent increase in open eye responses (Kaneko et al., 2008).

In the present study, we examined the role of homeostatic plasticity in the development and plasticity of sound representations in the TNF-α KO mouse. KO mice raised in the typical animal room environment had highly variable cortical frequency maps, often showing incomplete representation of the mouse-hearing frequency range. Although both WT and KO mice developed enlarged representations of a repeatedly exposed tone, they showed opposite effects as a result of multi-frequency exposure—narrowed frequency tuning in WT mice and broadened frequency tuning in KO mice. These results suggest that homeostatic plasticity may be involved in normal development and competitive refinement of acoustic representation in the primary auditory cortex.

3.3 Methods

Acoustic Exposure

All procedures used in this study were approved by the UC Berkeley Animal Care and Use Committee. Litters of juvenile TNF-α KO mice (KO) and corresponding C75Bl/6 wild-type mice (WT) from the Jackson Laboratory together with the nursing females were assigned to one of the 3 groups—a tone-exposure group, an enriched environment group, and a control group. The two experimental groups were repeatedly exposed to 1 s long trains of 6 tone pips (100 ms, 65 dB sound pressure level (SPL), 5-ms on and off cosine-squared ramps), with one train occurring every 2 s. The frequency of the tone pips within a train was the same, and was either fixed at 25 kHz for the tone-exposure group or randomly chosen from a continuum that ranged from 4 to 45 kHz for the enriched environment group. For this group, the acoustic power of the exposure sounds was uniformly distributed along the logarithmic frequency axis from 4 to 45 kHz (e.g. the power in the 4-8 kHz range is the same as in 8-16 kHz range). Sounds were generated with a National Instrument I/O card at a sampling rate of 200 kHz, amplified, and played through a calibrated speaker in a sound-attenuation

chamber where the animals were housed. The sound exposure started on postnatal day 9 (P9) and ended immediately before electrophysiological examination was conducted, typically on P19 to P21. Both sound exposed groups were compared with the control group, which were maintained in regular animal rooms and were mapped during the same period as the 2 experimental groups. The acoustic environment of the animal room is dominated by ambient low-level noise. Constant, broadband sounds at such low levels cannot mask sensory input. In addition, unmodulated sounds are ineffective in shaping sensory representations (Kim and Bao, 2009).

Electrophysiological Recording Procedure

The primary auditory cortex (AI) in naïve and sound-exposed KO and WT mice was mapped as previously described (Kim and Bao, 2009). Mice were anesthetized with Ketamine (100 mg/kg, IP) and xylazine (10 mg/kg, IP), and placed on a homeothermic heating pad at 36.5°C (Harvard Apparatus) in a sound attenuation chamber. The head was secured with a custom head-holder that left the ears unobstructed. The right auditory cortex was exposed and kept under a layer of silicone oil to prevent desiccation. Multi-unit activity was evenly sampled from primary auditory cortex. AI in both WT and KO mice was found consistently underneath the caudal half of the temporal-parietal bone suture. It can be identified by its tonotopic orientation—higher frequencies are represented more rostrally and slightly more dorsally. Other auditory cortical fields have different tonotopic orientations (Guo et al., 2012). The border of AI was defined by unresponsive sites or sites whose CFs were incongruent with the AI tontopic gradient. Because KO mice tended to have incomplete representations of low and high frequencies (Fig. 1), we carefully searched for those representations near the rostral and caudal ends of AI in both WT and KO mice, while maintaining the same sampling density. Typical sampling extent and density is shown in the map from animal 3 in Figure 1A. Neural responses were recorded using tungsten microelectrodes (FHC) at a depth of 400-450 μm, presumably from the thalamorecipient layer. Responses to 25-ms tone pips of 41 frequencies (4-64 kHz, 0.1 octave spacing) and 8 sound pressure levels (10-80 dB, 10-dB steps) were recorded to reconstruct the frequency-intensity-receptive field. A Tucker-Davis Technologies coupler model electrostatic speaker was used to present all acoustic stimuli into the left ear (contralateral to the recorded cortical hemisphere). Each frequency × intensity combination was repeated 3 times.

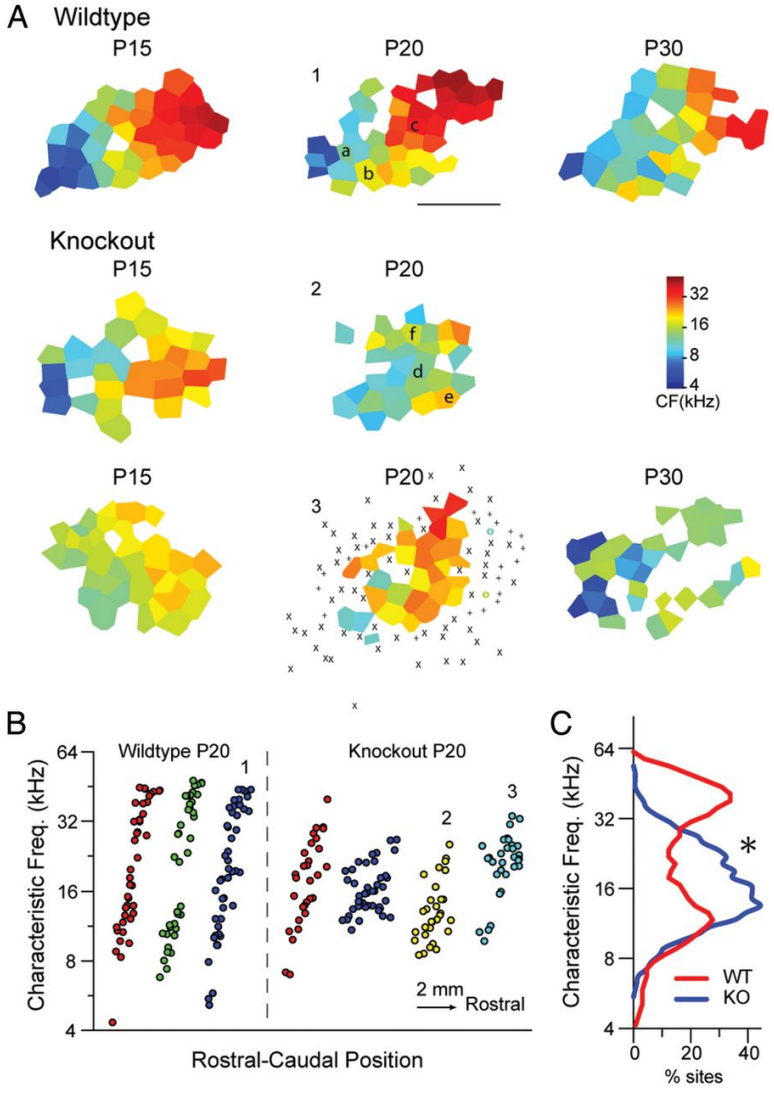

Figure 1. Development of cortical frequency map is impaired in TNF-α KO mice. (A) Example frequency maps at P15, P20, and P30 from WT and TNF-α KO mice. Receptive fields recorded at locations a-f are shown in Figure 2. The scale bar is 1 mm long and applies to all maps. The map from animal number 3 shows typical sampling density and extent. +, unresponsive sites where neural responses were visually examined but not recorded; x, unresponsive sites where neural responses were recorded; o, responsive sites where CF was incongruent with AI tonotopy. (B) Representative distributions of neuronal CFs along rostral-caudal axis recorded from 8 animals at P20. Note that the KO maps had more sites without an identifiable receptive field as indicated by the white regions within the maps. In addition, the represented frequency ranges were narrower and more variable in the KO mice. Plots marked with 1-3 were from the three P20 animals whose maps are shown in (A). (C) Percent of sites representing frequencies (±0.3 octaves). * indicates a statistically significant difference.

Data Analysis

The receptive fields and response properties were isolated using custom-made programs. First, the peri-stimulus time histogram (PSTH) was generated from responses to all 328 (41 frequencies × 8 intensities) tone pips, with 1-ms bin size (Fig. 4E). The mean firing rate was calculated for each bin and smoothed with a 5-point mean filter. The multiunit spontaneous firing rate was taken as the mean firing rate in the 50-ms window prior to stimulus onset. Peak latency was defined as the time to the peak PSTH response between 7 and 50 ms after the stimulus onset. The response window was defined as the period encompassing the PSTH peak, in which the mean firing rate in every bin was higher than baseline firing rate. The onset latency was defined at the onset of the response window. The tone-evoked response was measured as the maximum firing rate within the response window. Spikes that occurred within the response window were counted to reconstruct the receptive field.

The tuning curve contour was determined using a smoothing and thresholding algorithm. The response magnitude was plotted in the frequency-intensity space, and smoothed with a 3 × 3 mean filter (see Fig. 2B for examples). It was then thresholded at 28% of the maximum value of the smoothed response magnitude. Response areas smaller than 5 pixels were removed. The contour of the suprathreshold area was defined as the tuning curve. The raw responses in the suprathreshold area were defined as the isolated receptive field. The threshold of the neuron was the lowest sound level that elicited responses in the isolated receptive field. The characteristic frequency (CF) of a neuron was defined as the center of mass of the isolated receptive field for the 2 lowest suprathreshold sound levels. The center of mass CF was defined as (Ri fi)/Ri, in which Ri is the response magnitude to the ith tone with frequency fi, and responses were collapsed across the 2 sound levels. The maximum RF response was the maximum number of spikes activated by a single frequency-intensity combination. The mean RF response was the mean number of spikes for all frequency-dB combinations within the receptive field. Since each frequency-intensity combination was repeated 3 times, the average of those 3 responses was taken. Tuning bandwidth (BW) was defined as the BW of the receptive field at the specified intensity. We quantified BW at 80, 70, and 60 dB, but not at lower SPLs because many neurons did not respond at those low levels. To more accurately quantify BW at low SPLs, we measured BW at 10, 20, and 30 dB above the threshold. The receptive field size was the number of frequency-intensity combinations within the receptive field.

Auditory cortical map was reconstructed by Voronoi tessellation of the AI space and assigning response properties of a recording site to the corresponding polygon.

Statistics

Unless otherwise stated, statistical significance was determined with ANOVAs with post hoc Bonferroni's test.

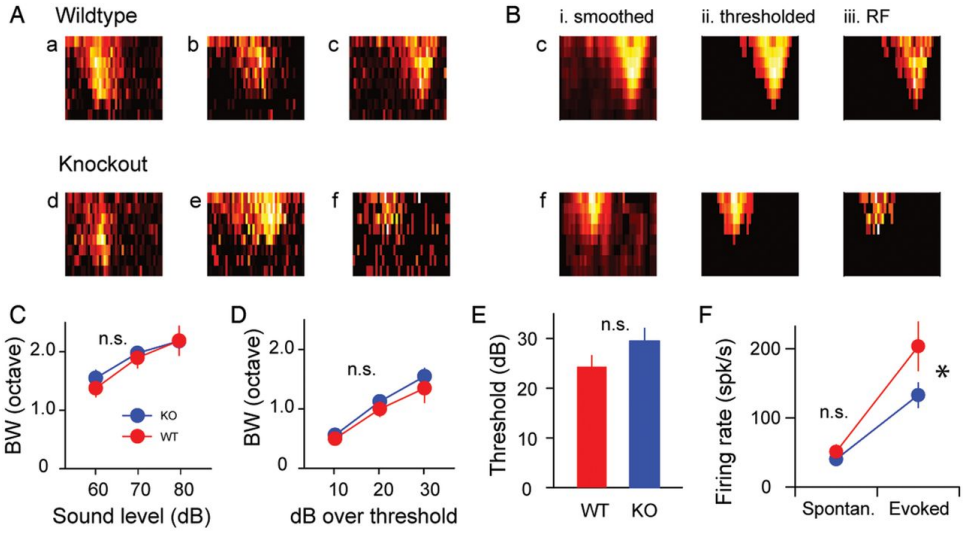

Figure 2. Cortical response properties are altered in TNF-α KO mice. (A) Example receptive fields recorded from WT and KO at P20. The recording sites are indicated in Figure 1. Horizontal axis depicts frequencies 4-64 kHz on a logarithmic scale. Vertical axis depicts intensity 0-70 dB with 10 dB steps. (B) Illustration of the method for automatically identifying receptive fields through smoothing and thresholding of responses in the frequency-intensity space. See Materials and Methods for details. (C and D) Tuning BWs were not altered in KO mice. (E) Stimulus threshold was not altered in KO mice. (F) Overall firing rates were reduced in KO mice. * indicates a statistically significant difference; n.s. signifies not significant.

3.4 Results

Development of Cortical Frequency Representations Is Impaired in TNF-α KO Mice

We examined the development of sound representations in the primary auditory cortex of KO and WT mice by mapping frequency-intensity representations at 3 ages: postnatal day 15 (P15), P20, and P30. The basic characteristics of sound representations observed in AI of WT mice in the present study (including tonotopic organization, frequency range, tuning BW, intensity threshold, and response latency; see figures below) were consistent with those reported before (ibid.). By P15, the WT mice had already developed finely topographic representations of nearly the full range of frequencies from 4 to 50 kHz persisting through P30 (Fig. 1A). In contrast, the frequency map in KO mice was more variable throughout the developmental window from P15 to P30 (Fig. 1A2). AI in KO mice generally represented a narrower frequency range than that in WTs (WT, $n = 8$, 2.9 ±0.1 octaves; KO, $n = 11$, 1.8±0.1 octaves; ANOVA, $F_{1,17} = 35.07$, $p < 0.00002$) often concentrated in the middle of the hearing range (Fig. 1). In P20 animals, there were more sites representing a middle frequency

range of 8-30 kHz in KO mice than WT mice (WT, 75/130; KO, 166/176; $\chi^2(1) = 56.96$, $p < 0.0001$; Fig. 1C).

Receptive field characterization indicated that tuning BW was not altered in KO (n = 5) compared with WT mice (n = 6; BW at 60-80 dB, 2-way repeated-measures ANOVA, genotype effect $F_{1,9} = 0.16$, $p = 0.70$, interaction $F_{2,18} = 0.48$, $p = 0.63$; BW10-30, genotype, $F_{1,9} = 0.56$, $p = 0.47$, interaction $F_{2,18} = 0.39$, $p = 0.68$; Fig. 2A-D). Although KO-receptive fields tended to have higher thresholds than those of WT, the effect was not significant ($F_{1,9} = 3.47$, $p = 0.095$; Fig. 2E). While no significant difference was found in spontaneous firing rate between WT and KO ($F_{1,9}$=2.31, $p = 0.16$), the tone-evoked firing rate was significantly higher in WT than in KO mice ($F_{1,9}$=5.36, $p = 0.046$; Fig. 2F).

TNF-α KO Mice Exhibit Single-Frequency Exposure-Induced Map Reorganization

We exposed both KO (n = 4) and WT (n = 4) mice to a 25-kHz tone repeated from P9 to P20, and examined sensory exposure-induced changes in cortical frequency representations. Exposure significantly increased the number of sites representing the frequency range of 25 kHz ± 0.3 octaves in both WT (naïve, 16/130; exposed, 68/163; 2 (1) = 30.59, $p < 0.0001$) and KO (naïve, 43/176; exposed, 70/150; 2 (1) = 17.68, $p < 0.0001$), indicating that KO mice undergo normal single-frequency exposure-induced map reorganization (Fig. 3). While single-frequency exposure did not alter the range of frequencies represented in AI of WT (2.9 ±0.2 octaves, compared with naïve WT at 2.9 ±0.1 octaves), it increased the AI frequency range in KO mice (2.7 ±0.2 octaves, compared with naïve KO at 1.8 ±0.1 octaves; ANOVA, $F_{3,23} = 15.36$, $p < 0.0001$; post hoc: naïve KO vs. exposed KO, $p = 0.0002$; naïve WTs vs. exposed WTs, $p = 0.97$; naïve WT vs. exposed KO., $p = 0.46$).

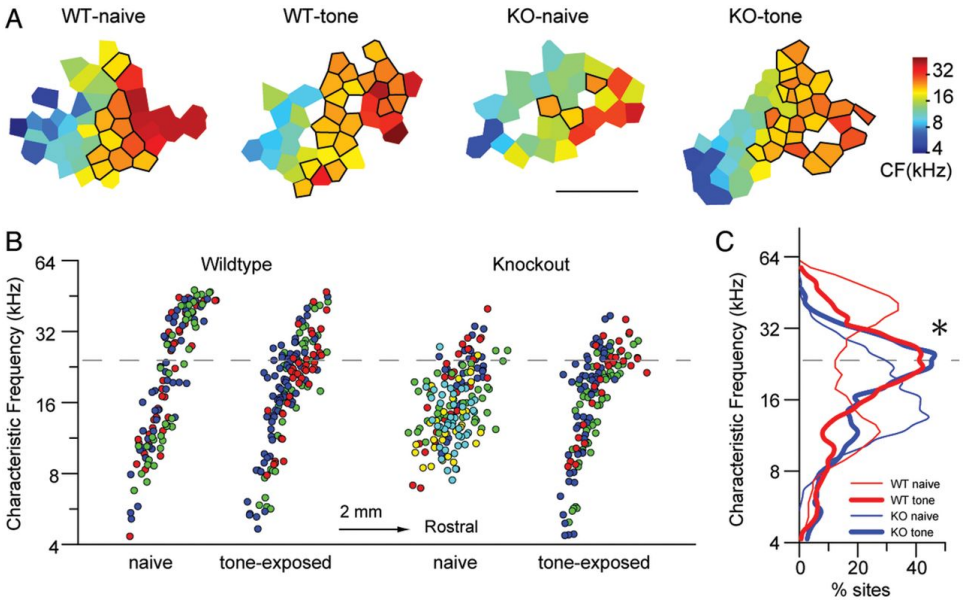

Figure 3. Single-frequency exposure-induced map reorganization is unimpaired in KO mice. (A) Example maps recorded from naïve and tone-exposed WT and KO mice at P20. Note the enlarged representations near 25 kHz, the exposure frequency, in exposed WT and KO animals. The scale bar is 1 mm long and applies to all maps. (B) Representative CF distributions along the rostral-caudal axis. (C) Percent of sites representing frequencies (±0.3 octaves). * indicates a statistically significant difference.

Single-frequency exposure had limited effects on receptive field and neuronal firing properties. Receptive field analysis indicates that single-frequency exposure did not alter overall tuning BWs of AI units (experience × genotype × intensity ANOVA with repeated measures for BW at 60-80 dB SPL, experience, $F_{1,15} = 0.007$, $p = 0.93$, genotype, $F_{1,15} = 1.85$, $p = 0.19$, interaction, $F_{1,15} = 0.94$, $p = 0.35$; ANOVA for BW10-30, experience, $F_{1,15} = 3.29$, $p = 0.09$, genotype, $F_{1,15} = 3.22$, $p = 0.09$, interaction, $F_{1,15} = 0.003$, $p = 0.96$; Fig. 4A,B). The receptive field size was not altered (genotype × experience ANOVA, genotype, $F_{1,15} = 0.001$, $p = 0.98$, experience, $F_{1,15} = 0.18$, $p = 0.90$; Fig. 4C).

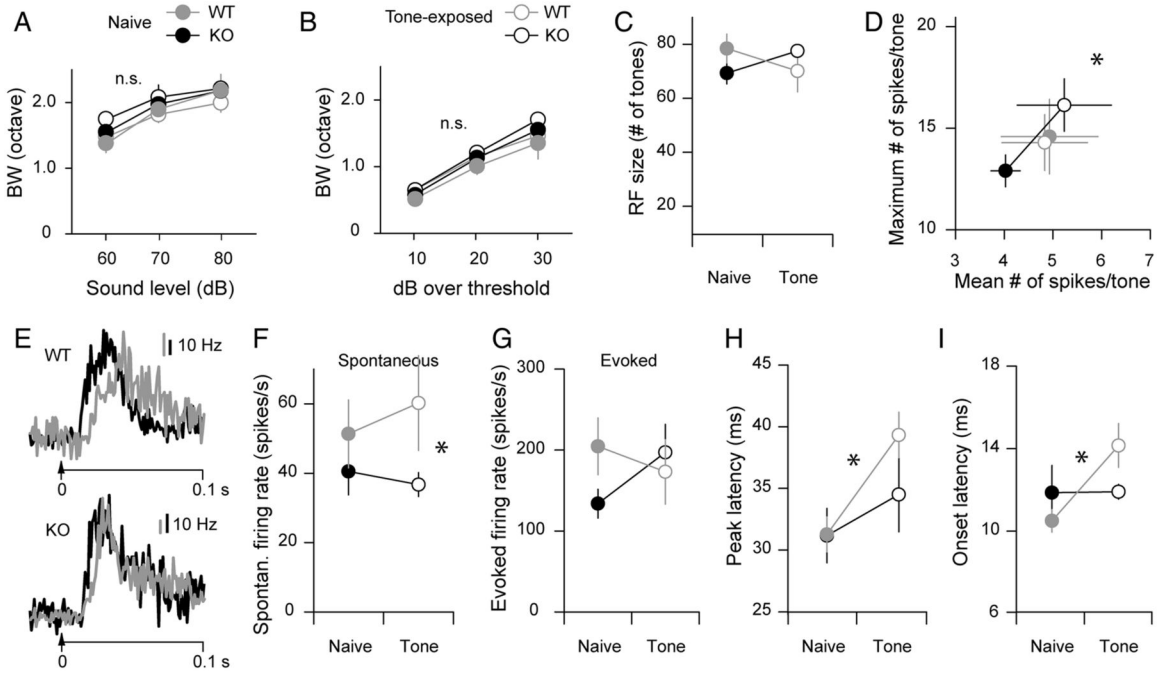

Figure 4. Effects of single-frequency exposure on cortical response properties in WT and TNF-α KO mice. (A-C) The single-frequency exposure did not change tuning BWs or receptive field sizes in WT or KO. (D) Mean and maximum response magnitudes to tones within the receptive field were increased in KO, but not in WT. (E) Examples of raw peri-stimulus histograms from naïve (black) and tone-exposed animals (gray). Note that the onset and peak of the tone-evoked responses were delayed in tone-exposed WT. (F) Although the spontaneous firing rate was generally higher in the WT than in KO, no exposure effects were observed. (G) Single-frequency exposure did not change the tone-evoked firing rate in either group. (H and I) Onset and peak latencies were increased in WT but not in KO. Asterisk indicates a statistically significant difference; n.s. signifies not significant.

We quantified mean and maximum response magnitude in the receptive field (for details, see Materials and Methods). Maximum response magnitude is the maximum number of spikes activated by any stimulus used to characterize the receptive field—that is, it measures response of a unit to its best stimulus. Mean response magnitude measures the overall responsiveness of the unit. The single-frequency exposure had different effects on KO and WT mice, enhancing responses in KO but not in WT (genotype × experience × type of response ANOVA, genotype × experience interaction, $F_{1,32} = 4.15$, $p = 0.0498$; Fig. 4D). We separated recorded units by their CFs—those with CFs $\geq$ 16 kHz and those with CFs<16 kHz. Neurons with CFs $\geq$ 16 kHz were more likely to be activated by the 25-kHz exposure tone than neurons with CFs<16 kHz (Fig. 3B). The maximum response magnitude was greater for tone-exposed KO mice than naïve KO mice only for units with high CFs (CFs $\geq$ 16 kHz) (F1, 7 = 10.23, $p = 0.015$), but not those with low CFs (CFs<16) kHz (F1, 7 = 1.70, $p = 0.233$). There was no difference between naïve and tone-exposed KO mice in mean

response magnitude in either of the CF groups (CFs $\geq$ 16 kHz: F1, 7 = 2.28, $p = 0.174$; CFs<16 kHz: F1, 7 = 0.775, $p = 0.408$). We also separately analyzed high-CF and low-CF units recorded from naïve and tone-exposed WT mice, and found no significant difference in maximum or mean response magnitude (CFs $\geq$ 16 kHz: maximum response magnitude, F1, 8 = 0.891, $p = 0.373$, mean response magnitude, F1, 8 = 0.150, $p = 0.709$; CFs $\geq$ 16 kHz: maximum, F1, 8 = 0.169, $p = 0.692$, mean, F1, 8 = 0.024, $p = 0.880$).

We constructed PSTH with responses to all 328 (41 frequencies $\times$ 8 intensities) tone pips (Fig. 4E) to extract spontaneous and evoked firing rates, and onset and peak response latencies. Whereas the spontaneous firing rate was generally higher in WT versus KO mice (genotype $\times$ experience ANOVA, genotype effect, $F_{1,17} = 5.264$, $p = 0.035$; Fig. 4F), it was not altered by single-frequency exposure (experience effect, $F_{1,17} = 0.048$, $p = 0.83$). The tone-evoked firing rate was not different between WT and KO mice, nor between naïve and tone-exposed mice (genotype, $F_{1,17} = 0.61$, $p = 0.45$; experience, $F_{1,17} = 0.47$, $p = 0.50$; Fig. 4G). We also separately analyzed effects of tone-exposure for units with CFs $\geq$ 16 kHz and those with CFs $<$ 16 kHz, but did not find statistically significant differences between naïve and tone-exposed mice, in either WT or KO group, for either spontaneous or tone-evoked firing rates (data not shown).

Single-frequency exposure delayed the onset and peak latencies of tone-evoked responses in WT but not in KO mice (onset latency: experience, $F_{1,15} = 5.70$, $p = 0.031$; post hoc WTs, $p = 0.002$; KOs, $p = 0.98$; Fig. 4H; peak latencies: experience, $F_{1,15} = 10.87$, $p = 0.0049$; post hoc, WT, $p = 0.0009$; KO, $p = 0.33$; Fig. 4I). A similar finding has been reported before (Engineer et al., 2004), but the neural mechanisms underlying the slower tone-evoked responses are unknown. Because each frequency-intensity combination was played only 3 times, we do not have enough data to reliably estimate onset or peak latency for individual tones.

Multi-Frequency Exposure Refines Frequency Tuning in WT and Broadens Tuning in KO Mice

To explore competitive interactions between different frequency inputs, we exposed WT (n = 4) and KO (n = 5) mice to an enriched multi-frequency tonal environment, in which the tone frequency was randomly chosen every 2 s from a uniform distribution ranging from 4 to 45 kHz and played in trains of 6 pips at a rate of 6 Hz. Like single-frequency exposure, our enriched environment manipulation altered the range of frequency representations (ANOVA group difference, $F_{3,24} = 11.58$, $p < 0.0001$; Fig. 5C,D). Post hoc pairwise tests showed that exposure to the enriched environment expanded the represented frequency range in KO mice (compared with naïve KO mice, $p = 0.036$), but not in WT mice ($p = 0.18$). Even after exposure, the frequency range represented by KO mice was still significantly narrower than the range represented by naïve WT mice ($p = 0.017$). However, after exposure, the representation range was no longer different between WT and KO mice ($p = 0.36$).

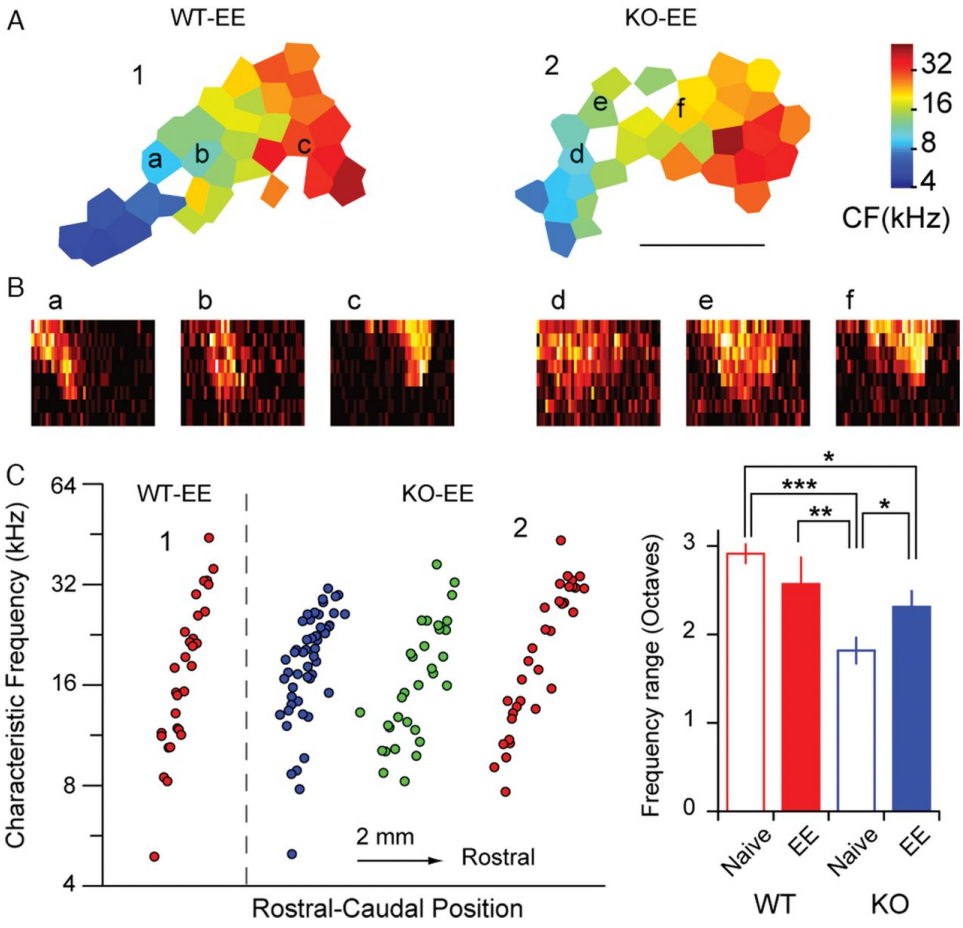

Figure 5. Multi-frequency-enriched acoustic environment increases the frequency range represented in KO mice. (A) Representative frequency maps of WT and KO mice exposed to enriched environments (EEs). (B) Representative receptive fields recorded from locations marked on cortical maps in (A). Horizontal axis: 4-64 kHz on a logarithmic scale. Vertical axis: 0-70 with 10 dB steps. (C) Representative distributions of CF on the trostral-caudal axis. Plots 1 and 2 correspond to the 2 maps in (A). (D) Frequency range represented by AI of WT and KO mice that were either naïve or exposed to enriched environments. $^{*}p < 0.05$; $^{**}p < 0.005$; $^{***}p < 0.001$.

Exposure to the multi-frequency-enriched environment resulted in narrower frequency tuning in WT mice and broader tuning in KO mice measured at 60-80 dB sound intensity levels (repeated-measures ANOVA, genotype × experience interaction, $F_{1,17} = 15.22$, $p = 0.0011$; post hoc, exposed WT vs. all other groups, $p < 0.03$; exposed KO vs. all other groups, $p < 0.05$) and at 10-30 dB above the threshold (interaction, $F_{1,17} = 14.03$, $p = 0.0016$; post hoc, exposed KO vs. 2 WT groups, $p < 0.01$; Figs 5 and 6A,B). Consistent with the altered tuning BW, we also observed reduced receptive field sizes in WT but not in KO (genotype × experience interaction, $F_{1,17} = 9.17$, $p = 0.0076$; post hoc, exposed WT vs. naïve WT, $p = 0.0048$; exposed WT vs. exposed KO, $p = 0.0061$; Fig. 6C). The

broadened tuning in exposed KO mice did not result in enlarged receptive field size, possibly because their threshold was slightly but not significantly increased. These results suggest that exposure to tones of different frequencies results in a winner-take-all type of competitive refinement of frequency representation in WT mice, which was impaired in KO mice lacking homeostatic plasticity.

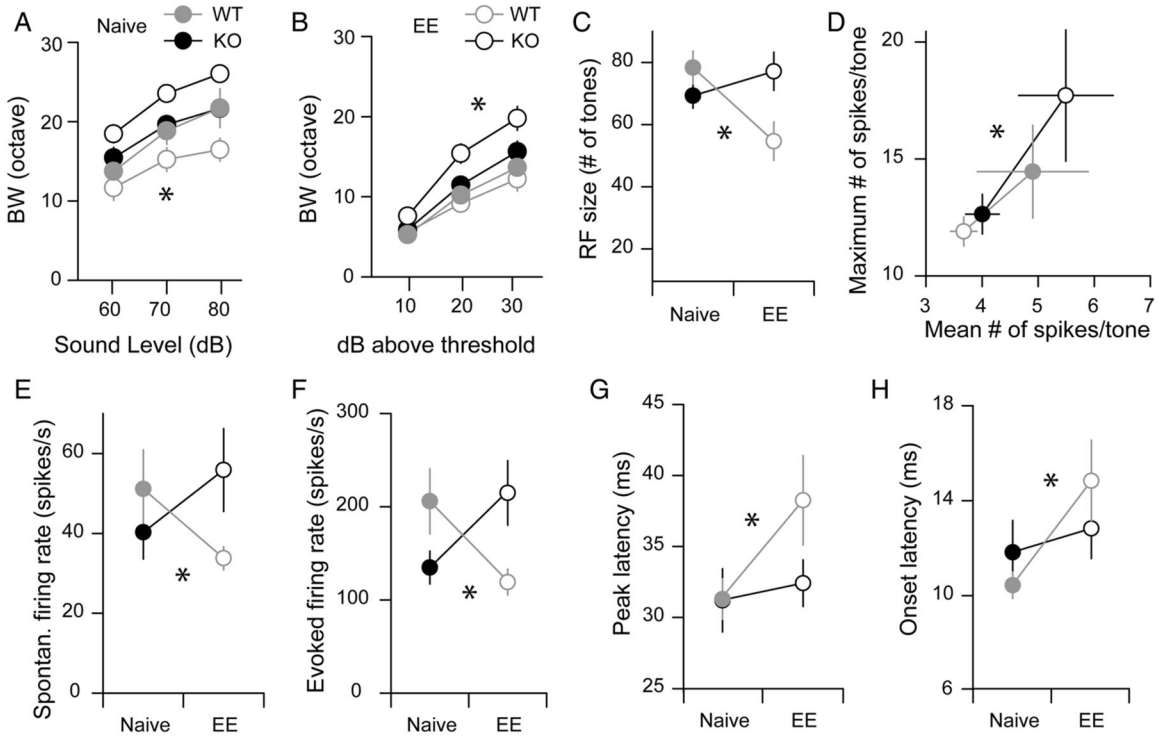

Figure 6. Effects of multi-frequency-enriched environment on cortical response properties in WT and KO mice. (A and B) Tuning BW narrowed in WT, but broadened in KO mice. (C) The receptive field size was reduced in WT, but unaltered in KO mice. (D-E) Spontaneous and tone-evoked firing rates were decreased in WT but increased in KO mice. (F) Mean and maximum response magnitudes to tones within the receptive field were increased in KO, but decreased in WT. (G and H) Onset and peak latencies were increased in WT but not in KO. Asterisk indicates a statistically significant difference.

KO Mice Are Impaired in Homeostatic Regulation of Cortical Responses

Overstimulation of AI with a wide range of frequencies resulted in a lower neuronal firing rate compared with naïve WT mice (spontaneous firing rate, $F_{1,10} = 5.13$, $p = 0.047$; tone-evoked, $F_{1,10} = 5.71$, $p = 0.038$; Fig. 6E,F), which may be considered a type of in vivo homeostatic

regulation of neuronal activity by sensory experience (see Discussion). However, exposed KO mice showed a greater tone-evoked firing rate compared with naïve KO mice (tone-evoked, $F_{1,8} = 5.54$, $p = 0.046$; Fig. 6D). Spontaneous firing rate also trended higher in the exposed KO mice, although the effect was not significant ($F_{1,8} = 1.99$, $p = 0.19$; Fig. 6D). A comparison of mean and maximum responses in the receptive field confirmed the above observations, showing that exposure to the multi-frequency-enriched environment lowered AI responses in WT while increasing responses in KO mice (genotype × experience × response ANOVA, experience, $F_{1,36} = 4.91$, $p = 0.033$; Fig. 6F). Like single-frequency exposure, the multi-frequency exposure also delayed onset and peak latencies in WT but not in KO mice (onset latency: experience, $F_{1,17} = 6.36$, $p = 0.022$; post hoc WTs, $p = 0.0091$; KOs, $p = 0.93$; Fig. 6G; peak latencies: experience, $F_{1,17} = 4.98$, $p = 0.039$; post hoc, exposed WT vs. all other groups, $p < 0.04$; Fig. 6H). Instead of responding to overstimulation with a homeostatic decrease in neural activity, KO mice displayed an increase in responses indicating an absence of homeostatic processes.

3.5 Discussion

We have compared the development and sound-induced reorganization of sound representations in AI of TNF-α KO mice and their WT controls. Our results indicate that, compared with WT mice, KO mice 1) develop more variable and incomplete frequency representations, 2) have weaker cortical responses to tones, 3) exhibit normal expansion of cortical representations in response to single-frequency, repeated tone exposure, 4) show enhanced cortical responses after sensory over-stimulation, 5) and do not show competitive refinement of frequency representations after exposure to multifrequency tones. These results suggest that TNF-α and its associated cellular processes are important in cortical response gain control and competitive refinement of cortical acoustic representations.

The mammalian auditory cortex evolved to be highly adaptive, such that it overrepresents prevalent and salient environmental sounds within the acoustic environment (**Edeline1999**; Diamond and Weinberger, 1986; Gonzalez-Lima and Scheich, 1986; Ohl and Scheich, 1996; Pantev et al., 1998; Gao and Suga, 2000; Zhang, Bao, and Merzenich, 2001; Syka, 2002; Fritz et al., 2003; Mrsic-Flogel, Schnupp, and King, 2003; Dean, Harper, and McAlpine, 2005; Popescu and Polley, 2010; Cohen, Rothschild, and Mizrahi, 2011; Takahashi et al., 2011). However, adaptation to some sounds may impair subsequent learning of new sounds in the future (Sarro and Sanes, 2011). Therefore, it is important to strike a balance between plasticity and stability. The acoustic environment can be highly variable. For example, while the acoustic environment of a typical animal room may be considered impoverished, it can be dramatically enriched locally by conspecific vocalizations (Kim and Bao, 2009; Grimsley, Monaghan, and Wenstrup, 2011). Species-specific vocalizations often occur in a high-frequency range, whereas sounds in the natural environment have more power in the lower frequency range (Liu et al., 2003; Kim and Bao, 2009). In addition, animals are typically more sensitive to certain frequencies in their hearing range. Experimental evidence

indicates that, in spite of the environmental variability and hearing constraints, the auditory cortex more or less consistently represents a large range of hearing frequencies (e.g. see WT cortical map in Fig. 1). This stability appears to break down in TNF-α KO mice, which display narrower ranges and more variability in their frequency representations. This impairment seems to be the result of impoverished sensory experience, as it is reversed by repeated acoustic exposure to single or multiple tones. It is conceivable that WT animals maintain stable acoustic representations in an impoverished sensory environment by enhancing input connectivity in the understimulated sensory pathways through homeostatic mechanisms. In animals with deficient homeostatic plasticity but normal Hebbian plasticity, cortical representations may be dictated to a greater degree by the highly variable acoustic environment, leading to impaired frequency representation as we observed in KO mice. It should be noted that no differences in retinotopy or basal visual response were observed in the primary visual cortex (VI) of the TNF-α KO (Kaneko et al., 2008). The different effects of TNF-α KO on basal stimulus representations in AI versus VI could be due to the fact that the visual stimulation is more uniform in the retinocentric visual space, whereas auditory stimulation is highly variable in the frequency space as we have discussed above.

The lack of homeostatic regulation in KO mice was also evident in the magnitude of cortical responses. Cortical responses to tone pips were weaker in naïve KO than in naïve WT mice, which again could be attributed to the acoustically impoverished housing environment. More telling evidence comes from the finding that, after repeated exposure to the multifrequency enriched environment, cortical responses in WT mice were reduced. Presumably, this occurs through homeostatic processes, whereas cortical responses in KO mice are enhanced through Hebbian plasticity. This is also consistent with the previous findings that TNF-α KO mice have normal LTP (Albensi and Mattson, 2000; Stellwagen and Malenka, 2006; Kaneko et al., 2008).

Refinement of neuronal connectivity requires competitive synaptic interactions, and theoretical considerations suggest that homeostatic plasticity may be involved in such interactions (Davis and Bezprozvanny, 2001; Burrone and Murthy, 2003; Turrigiano and Nelson, 2004). Recent experimental studies examined competitive interactions in TNF-α KO mice by blocking the activity of a subset of sensory input through monocular deprivation. The results support a role of homeostatic plasticity underlying the competitive component of ocular dominance plasticity (Kaneko et al., 2008; Ranson et al., 2012). In the present study, we examined competitive interaction using the opposite sensory manipulation—by overstimulation of all sensory input asynchronously. In WT mice, exposure to a multi-frequency environment resulted in narrower frequency tuning, indicative of competitive refinement of sensory representations. In contrast, the identical sensory manipulation resulted in broadened tuning in mice lacking TNF-α, suggesting that a TNF-α -mediated process, presumably homeostatic plasticity, is required for the refinement of frequency selectivity observed in WT mice. Our results support a role of homeostatic plasticity in competitive refinement of sensory representations and neuronal circuits.

As we have discussed above, the more variable and incomplete frequency representations in the AI of naïve KOs are likely due to impaired upregulation of sensory responses

in the understimulated pathways. This is consistent with the findings that TNF-α is required for homeostatic upregulation of excitatory synapses and downregulation of inhibitory synapses in hippocampal and cortical slices (Stellwagen and Malenka, 2006; Kaneko et al., 2008). Our observation of impaired competitive interaction in the overstimulated TNF-α KO mice suggests that over activation-induced homeostatic downregulation of excitatory synapses and/or upregulation of inhibitory synapses is disrupted in the KOs. Although electrophysiological studies indicate that TNF-α is not needed for homeostatic downregulation of excitatory synapses in hippocampal slices (Stellwagen and Malenka, 2006), it is unclear whether homeostatic upregulation of inhibitory synapses is normal in TNF-α KO mice. Such a mechanism can be induced by sensory overstimulation, suppressing cortical responses (Knott et al., 2002). Furthermore, the underlying mechanisms may be different between in vivo homeostatic plasticity following sensory stimulation and in vitro homeostatic plasticity after neuronal stimulation. It remains to be determined whether TNF-α KO mice are impaired in homeostatic plasticity following sensory deprivation or overstimulation in vivo. While TNF-α KO mice are impaired in some forms of homeostatic plasticity and normal in one form of LTP (Stellwagen and Malenka, 2006; Kaneko et al., 2008), they may well have other uncharacterized plasticity deficits that could lead to the observed impairments in the development and competitive refinement of sound representations in AI. Further characterization of different forms of synaptic plasticity in the TNF-α KO mice, and identification of the types of synaptic plasticity involved in experience-dependent cortical development and refinement, may shed new light on how TNF-α is involved in those processes.

In the present study, we focused on 2 cortical plasticity effects observed in WT mice: single-frequency exposure-induced expansion of cortical representations at the exposure frequency and multifrequency exposure-induced reduction of cortical response magnitude (Condon and Weinberger, 1991; Zhang, Bao, and Merzenich, 2001; Pienkowski and Eggermont, 2012). Frequency map expansion appears to involve Hebbian-type, LTP-like potentiation of excitatory synapses (Froemke, Merzenich, and Schreiner, 2007; Sun et al., 2010). The mechanism underlying sound exposure-induced response reduction is largely unknown. We considered it a type of homeostatic regulation of cortical activity (which is different from homeostatic synpatic plasticity) purely based on its impact at the level of cortical activity. In WT mice, repetitive stimulation with multifrequency tones is likely to increase the overall level of cortical activity. The observed reduction of sound-evoked responses should dampen activity levels, and counterbalance the overstimulation of the auditory cortical neurons. In the present study, we defined homeostatic regulation of cortical responses as a reduction of cortical responses induced by sensory overstimulation, or an enhancement of responses caused by sensory deprivation. We found that in KO mice single-frequency exposure induced frequency map changes, but multifrequency exposure did not cause-response reduction, suggesting a role of TNF-α in homeostatic regulation of cortical activity.

The normal single-frequency exposure-induced map expansion, impaired multi-frequency exposure-induced tuning refinement, and differentially regulated cortical response patterns observed in the TNF-α KO mice indicate that multiple cellular mechanisms are at work in shaping cortical sensory representations and response properties Bear, 2003; Burrone

and Murthy, 2003; Turrigiano and Nelson, 2004; Dan and Poo, 2006; Liu et al., 2007; Wu et al., 2008; Feldman, 2009). Using genetic manipulations to target-specific cellular mechanisms, we may be able to dissect the circuits and cellular mechanisms involved in physiological and pathological plasticity. For example, both Hebbian plasticity-mediated sensory map changes and homeostatic plasticity-mediated changes in spontaneous firing rate are considered potential mechanisms underlying hearing loss-induced tinnitus and phantom pain (Eggermont, 2006; Yang et al., 2011). Further studies using TNF-α KO mice may help clarify the specific roles of those cellular mechanisms in pathological phantom perception.

Bibliography

Abbott, L F and S B Nelson (2000). "Synaptic plasticity: taming the beast." In: *Nature neuroscience* 3 Suppl, pp. 1178–1183.

Albensi, B C and M P Mattson (2000). "Evidence for the involvement of TNF and NF-kappaB in hippocampal synaptic plasticity." In: *Synapse (New York, N.Y.)* 35, pp. 151–159.

Bear, Mark F (2003). "Bidirectional synaptic plasticity: from theory to reality." In: *Philosophical transactions of the Royal Society of London. Series B, Biological sciences* 358, pp. 649–655.

Burrone, Juan and Venkatesh N. Murthy (2003). *Synaptic gain control and homeostasis*.

Chang, Edward F and Michael M Merzenich (2003). "Environmental noise retards auditory cortical development". In: *Science* 300, pp. 498–502.

Chang, Edward F et al. (2005). "Development of spectral and temporal response selectivity in the auditory cortex." In: *Proceedings of the National Academy of Sciences of the United States of America* 102, pp. 16460–16465.

Cohen, Lior, Gideon Rothschild, and Adi Mizrahi (2011). "Multisensory integration of natural odors and sounds in the auditory cortex". In: *Neuron* 72, pp. 357–369.

Condon, C D and N M Weinberger (1991). "Habituation produces frequency-specific plasticity of receptive fields in the auditory cortex." In: *Behavioral neuroscience* 105, pp. 416–430.

Crozier, Robert A et al. (2007). "Deprivation-induced synaptic depression by distinct mechanisms in different layers of mouse visual cortex." In: *Proceedings of the National Academy of Sciences of the United States of America* 104, pp. 1383–1388.

Dan, Yang and Mu-Ming Poo (2006). "Spike timing-dependent plasticity: from synapse to perception." In: *Physiological reviews* 86, pp. 1033–1048.

Davis, G W and I Bezprozvanny (2001). "Maintaining the stability of neural function: a homeostatic hypothesis." In: *Annual review of physiology* 63, pp. 847–869.

Dean, Isabel, Nicol S Harper, and David McAlpine (2005). "Neural population coding of sound level adapts to stimulus statistics." In: *Nature neuroscience* 8, pp. 1684–1689.

Desai, Niraj S et al. (2002). "Critical periods for experience-dependent synaptic scaling in visual cortex." In: *Nature neuroscience* 5, pp. 783–789.

Diamond, D M and N M Weinberger (1986). "Classical conditioning rapidly induces specific changes in frequency receptive fields of single neurons in secondary and ventral ectosylvian auditory cortical fields." In: *Brain research* 372, pp. 357–360.

Eggermont, J J (2006). "Cortical tonotopic map reorganization and its implications for treatment of tinnitus." In: *Acta oto-laryngologica. Supplementum*, pp. 9–12.

Engineer, Navzer D et al. (2004). "Environmental enrichment improves response strength, threshold, selectivity, and latency of auditory cortex neurons." In: *Journal of neurophysiology* 92, pp. 73–82.

Feldman, Daniel E (2009). "Synaptic mechanisms for plasticity in neocortex." In: *Annual review of neuroscience* 32, pp. 33–55.

Frenkel, Mikhail Y. and Mark F. Bear (2004). "How monocular deprivation shifts ocular dominance in visual cortex of young mice". In: *Neuron* 44, pp. 917–923.

Fritz, Jonathan et al. (2003). "Rapid task-related plasticity of spectrotemporal receptive fields in primary auditory cortex." In: *Nature neuroscience* 6, pp. 1216–1223.

Froemke, Robert C, Michael M Merzenich, and Christoph E Schreiner (2007). "A synaptic memory trace for cortical receptive field plasticity." In: *Nature* 450, pp. 425–429.

Fu, Yu-Xi et al. (2002). "Temporal specificity in the cortical plasticity of visual space representation." In: *Science (New York, N.Y.)* 296, pp. 1999–2003.

Gao, E and N Suga (2000). "Experience-dependent plasticity in the auditory cortex and the inferior colliculus of bats: role of the corticofugal system." In: *Proceedings of the National Academy of Sciences of the United States of America* 97, pp. 8081–8086.

Goel, Anubhuthi and Hey-Kyoung Lee (2007). "Persistence of experience-induced homeostatic synaptic plasticity through adulthood in superficial layers of mouse visual cortex." In: *The Journal of neuroscience : the official journal of the Society for Neuroscience* 27, pp. 6692–6700.

Gonzalez-Lima, Francisco and Henning Scheich (1986). "Neural substrates for tone-conditioned bradycardia demonstrated with 2-deoxyglucose. II. Auditory cortex plasticity". In: *Behavioural Brain Research* 20.3, pp. 281–293.

Grimsley, J. M S, J. J M Monaghan, and Jeffrey J. Wenstrup (2011). "Development of social vocalizations in mice". In: *PLoS ONE* 6.

Guo, W. et al. (2012). *Robustness of Cortical Topography across Fields, Laminae, Anesthetic States, and Neurophysiological Signal Types*.

Han, Yoon K et al. (2007). "Early experience impairs perceptual discrimination." In: *Nature neuroscience* 10, pp. 1191–1197.

Heynen, Arnold J et al. (2003). "Molecular mechanism for loss of visual cortical responsiveness following brief monocular deprivation." In: *Nature neuroscience* 6, pp. 854–862.

Hou, Qingming et al. (2008). "Homeostatic regulation of AMPA receptor expression at single hippocampal synapses." In: *Proceedings of the National Academy of Sciences of the United States of America* 105, pp. 775–780.

Insanally, Michele N, Badr F Albanna, and Shaowen Bao (2010). "Pulsed noise experience disrupts complex sound representations." In: *Journal of neurophysiology* 103, pp. 2611–2617.

Insanally, Michele N et al. (2009). "Feature-dependent sensitive periods in the development of complex sound representation." In: *The Journal of neuroscience : the official journal of the Society for Neuroscience* 29, pp. 5456–5462.

Kaneko, Megumi et al. (2008). "Tumor Necrosis Factor-α Mediates One Component of Competitive, Experience-Dependent Plasticity in Developing Visual Cortex". In: *Neuron* 58, pp. 673–680.

Kim, Heesoo and Shaowen Bao (2009). "Selective increase in representations of sounds repeated at an ethological rate." In: *The Journal of neuroscience : the official journal of the Society for Neuroscience* 29, pp. 5163–5169.

Knott, Graham W. et al. (2002). "Formation of dendritic spines with GABAergic synapses induced by whisker stimulation in adult mice". In: *Neuron* 34, pp. 265–273.

Liu, Bao-hua et al. (2007). "Defining cortical frequency tuning with recurrent excitatory circuitry." In: *Nature neuroscience* 10, pp. 1594–1600.

Liu, Robert C et al. (2003). "Acoustic variability and distinguishability among mouse ultrasound vocalizations." In: *The Journal of the Acoustical Society of America* 114, pp. 3412–3422.

Maffei, Arianna and Gina G Turrigiano (2008). "Multiple modes of network homeostasis in visual cortical layer 2/3." In: *The Journal of neuroscience : the official journal of the Society for Neuroscience* 28, pp. 4377–4384.

Malenka, Robert C. and Mark F. Bear (2004). *LTP and LTD: An embarrassment of riches.*

Mrsic-Flogel, Thomas D, Jan W H Schnupp, and Andrew J King (2003). "Acoustic factors govern developmental sharpening of spatial tuning in the auditory cortex." In: *Nature neuroscience* 6, pp. 981–988.

Mrsic-Flogel, Thomas D. et al. (2007). "Homeostatic Regulation of Eye-Specific Responses in Visual Cortex during Ocular Dominance Plasticity". In: *Neuron* 54, pp. 961–972.

Ohl, F W and H Scheich (1996). "Differential frequency conditioning enhances spectral contrast sensitivity of units in auditory cortex (field Al) of the alert Mongolian gerbil." In: *The European journal of neuroscience* 8, pp. 1001–1017.

Pantev, C et al. (1998). "Increased auditory cortical representation in musicians." In: *Nature* 392, pp. 811–814.

Pienkowski, Martin and Jos J. Eggermont (2012). *Reversible Long-Term Changes in Auditory Processing in Mature Auditory Cortex in the Absence of Hearing Loss Induced by Passive, Moderate-Level Sound Exposure.*

Popescu, Maria V. and Daniel B. Polley (2010). "Monaural Deprivation Disrupts Development of Binaural Selectivity in Auditory Midbrain and Cortex". In: *Neuron* 65, pp. 718–731.

Ranson, Adam et al. (2012). "Homeostatic plasticity mechanisms are required for juvenile, but not adult, ocular dominance plasticity." In: *Proceedings of the National Academy of Sciences of the United States of America* 109.4, pp. 1311–6.

Sarro, Emma C and Dan H Sanes (2011). "The cost and benefit of juvenile training on adult perceptual skill." In: *The Journal of neuroscience : the official journal of the Society for Neuroscience* 31, pp. 5383–5391.

Stellwagen, David and Robert C Malenka (2006). "Synaptic scaling mediated by glial TNF-alpha." In: *Nature* 440, pp. 1054–1059.

Sun, Yujiao J et al. (2010). "Fine-tuning of pre-balanced excitation and inhibition during auditory cortical development." In: *Nature* 465, pp. 927–931.

Syka, Josef (2002). "Plastic changes in the central auditory system after hearing loss, restoration of function, and during learning." In: *Physiological reviews* 82, pp. 601–636.

Takahashi, H. et al. (2011). "Learning-stage-dependent, field-specific, map plasticity in the rat auditory cortex during appetitive operant conditioning". In: *Neuroscience* 199, pp. 243–258.

Turrigiano, Gina G and Sacha B Nelson (2004). "Homeostatic plasticity in the developing nervous system." In: *Nature reviews. Neuroscience* 5, pp. 97–107.

Villers-Sidani, Etienne de et al. (2007). "Critical period window for spectral tuning defined in the primary auditory cortex (A1) in the rat." In: *The Journal of neuroscience : the official journal of the Society for Neuroscience* 27, pp. 180–189.

Wu, Guangying K. et al. (2008). "Lateral Sharpening of Cortical Frequency Tuning by Approximately Balanced Inhibition". In: *Neuron* 58, pp. 132–143.

Yang, Sungchil et al. (2011). "Homeostatic plasticity drives tinnitus perception in an animal model." In: *Proceedings of the National Academy of Sciences of the United States of America* 108, pp. 14974–14979.

Zhang, L I, Shaowen Bao, and M M Merzenich (2001). "Persistent and specific influences of early acoustic environments on primary auditory cortex." In: *Nature neuroscience* 4, pp. 1123–1130.

Zhang, L I et al. (1998). "A critical window for cooperation and competition among developing retinotectal synapses." In: *Nature* 395, pp. 37–44.

Zhou, X. et al. (2008). "Influences of un-modulated acoustic inputs on functional maturation and critical-period plasticity of the primary auditory cortex". In: *Neuroscience* 154, pp. 390–396.

Chapter 4

The role of TNF-α in tinnitus

4.1 Overview

4.2 Introduction

Tinnitus is the perception of sounds in the absence of acoustic stimuli. The potential causes of tinnitus are diverse, but the biggest risk factor is hearing loss. Previously research has indicated that hearing loss activates neural plasticity mechanisms in the central auditory pathway, which is widely believed to contribute to tinnitus (Roberts et al., 2010). Of particular interest is homeostatic plasticity—the capacity of a neuron to adjust its synaptic transmission and intrinsic membrane properties to maintain its overall level of activity (Turrigiano, 1999; Davis and Bezprozvanny, 2001). For example, when sensory input is weakened by hearing loss, neurons in the auditory pathway become more excitable by adjusting their synaptic strengths and intrinsic membrane properties through homeostatic plasticity (Kotak et al., 2005; Yang et al., 2011; Yang, Su, and Bao, 2012). Following noise-induced hearing lesion, the expression of glutamic acid decarboxylase (GAD), the enzyme that synthesizes inhibitory neural transmitter GABA, is down-regulated in the dorsal cochlear nucleus, inferior colliculus, and auditory cortex (Abbott et al., 1999; Milbrandt et al., 2000; Yang et al., 2011; Browne, Morley, and Parsons, 2012). Consequently, noise-induced hearing lesion results in reduced GABA release, reduced tonic inhibition and enhanced excitability in cortical pyramidal neurons (Yang et al., 2011; Yang, Su, and Bao, 2012). Down-regulation of GABAergic inhibition is considered a potential mechanism for tinnitus (Yang et al., 2011; Llano, Turner, and Caspary, 2012).

Tumor necrosis factor-α (TNF-α) is a pro-inflammatory cytokine that also plays an important role in homeostatic plasticity in the central nervous system (Stellwagen et al., 2005; Stellwagen and Malenka, 2006; Steinmetz and Turrigiano, 2010; Wang, Brozoski, and Caspary, 2011). For example, TNF-α sequestration with a soluble form of TNF receptor blocks TTX treatment-induced up-scaling of glutamate synapses in cultured neurons (Stellwagen and Malenka, 2006; Steinmetz and Turrigiano, 2010). Relevant to reduced neuronal inhibi-

tion as a potential tinnitus mechanism, TNF-α mediates TTX-induced down-regulation of GABAergic activity in vitro (Stellwagen and Malenka, 2006) by regulating endocytosis of GABA-A receptors (Stellwagen et al., 2005).

TNF-α is also involved in homeostatic modulation of central auditory neurons. Although TNF-α knockout mice have normal gross brain structure, Hebbian LTP (Kaneko et al., 2008) and tone-induced map reorganization (Yang et al., 2013), compared to wildtype controls, TNF-α knockout mice showed weaker cortical response to tones, suggesting that while wildtype mice can up-regulate cortical responses in the relatively impoverished acoustic environment of the vivarium, the knockout mice lacked such homeostatic plasticity (Yang et al., 2013). When acoustically over stimulated, wildtype mice showed homeostatic down regulation of cortical responses to sounds, while TNF-α knockout mice showed enhanced responses (ibid.), indicative of a lack of homeostatic regulation of cortical responses by the level of sensory input.

In the present study we examined the role of TNF-α in noise-induced tinnitus. We found that monaural hearing loss-induced aural dominance shift was largely absent in the KO mice. Wildtype but not TNF-α knockout mice developed tinnitus after monaural noise exposure. Infusion of recombinant mouse TNF-α protein into the auditory cortex resulted in tinnitus in both wildtype and TNF-α knockout mice without noise exposure.

4.3 Methods

Noise exposure and auditory brainstem response (ABR)

All experimental procedures were reviewed and approved by UC Berkeley Animal Care and Use Committee. TNF-α KO mice and corresponding C75Bl/6 WT mice were originally purchased from the Jackson Laboratory, and were bred in a UC Berkeley animal facility. Animals were anesthetized with ketamine (100 mg/kg, IP) and xylazine (10 mg/kg, IP), and maintained at 36.5C with a homeothermic heating pad (Harvard Apparatus). Unilateral noise-induced hearing loss (NIHL) were performed in a sound attenuation chamber by playing a continuous pure tone of 8 kHz at 112 dB SPL through a calibrated custom-made piezo earphone speaker to the left ear of the mouse for 2 hours, while the right ear was protected with sound attenuating clay. The sound level was calibrated with a Bruel and Kjaer 4135 condenser microphone (Nrum, Denmark) before and after the NIHL.

Hearing thresholds were assessed using auditory brainstem responses (ABR). ABR signals were recorded using the BioSigRP software on a TDT RX5 Sys3 recording rig. Tone pips (3-ms full-cycle sine waves at 4, 8, 16 and 32 kHz at 5-dB intensity steps from 0 to 70 dB) were delivered to the ears at a rate of 19 times per second through a calibrated TDT earphone, and 500 recordings were averaged to generate each ABR trace. ABR signals were recorded with three electrodes subcutaneously inserted behind the ear ipsilateral to the speaker, at the vertex of the head, and at the back of the body near the tail. The sound

level that activated a minimal discernable response was defined as the auditory threshold for the particular frequency for each ear.

Behavioral test of tinnitus with a gap detection task

Tinnitus was assessed using the gap detection paradigm (Turner et al., 2006). The gap detection task measures the acoustic startle response elicited by a brief white noise pulse and its suppression by a preceding silent gap embedded in a background sound. This paradigm has recently been confirmed to detect tinnitus in human subjects (Fournier and H??bert, 2013). Mice were placed in a small box, which rested atop a piezoelectric sensor within a sound attenuation chamber. Sounds were played through an open field speaker (FOSTEX FT17H) fixed above the small box. Each trial began with a carrier pure tone (frequency pseudorandomly selected from 5, 7, 10, 14, 20, 28, or 45 kHz, all at 75 dB SPL), played for 10-20 s. In uncued trials, the carrier tone was followed by a startle stimulus—a 50 ms white noise burst at 102 dB SPL. In cued trials, the startle stimulus was preceded by a 50 ms silence, 100 ms prior to its onset. In each testing session, the animal performed a total of 500 trials (50% cued and 50% uncued). After each session, we calculated the startle response ratio, which is defined as the average startle amplitude to the cued trials divided by the average amplitude of the uncued trials. The startle response ratio signifies a silent-gap induced reduction of the startle response. For example, a startle response ratio of 0.6 indicates a 40% reduction of the startle amplitude for the cued trials. A startle response ratio of 1 suggests that the animal failed to detect the silent gap.

To assess an animals ability to perform an auditory task, separate from its ability to detect a silent gap, the pre-pulse inhibition (PPI) task was administered in a separate group of mice immediately before and after (2 d and 10 d) NIHL. The physical setup for the PPI task was identical to that of the gap detection. However, the trial structure differed in that carrier tone was absent and a white noise burst was cued by a 50-ms pure tone pulse (frequency pseudorandomly selected from 5, 7, 10, 14, 20, 28, or 45 kHz, all at 75 dB SPL). In short, the PPI task tests an animals ability to detect a pure tone pulse in silence, while the gap detection task measures an animals ability to detect a silent gap in a continuous pure tone.

Mice were first acclimated to the testing chamber and trained until the behavior stabilized across two days. On average, 1000 trials were given prior to the first test session. We compared individual animals performance before and after the experimental manipulation. An increase of gap ratio accompanied by i) normal ABR for the intact ear and ii) normal PPI behavior were assumed to indicate tinnitus. Because both the gap detection task and the PPI task require normal hearing and hearing sensitivity above 32 kHz was highly variable across animals, only trials with carrier frequencies between 5 and 20 kHz were included in the final analysis.

Injection of recombinant TNF-α in the auditory cortex Mice were anaesthetized with ketamine (100 mg/kg IP) and xylazine (10 mg/kg IP). Injection was done stereotactically to the right auditory cortex. A burr hole was made on the temporal ridge 1.75 mm anterior

to the transverse suture. A pulled glass micropipette filled with recombinant mouse TNF-α (66.6 ng///textmul in 1% mouse albumin fraction V) or 1% mouse albumin fraction V solution was lowered to 500 /textmum below the pial surface and 1.5 l solution was injected at 100 nl/min by pressure injection (Stoelting Quintessential Injector, Wood Dale, IL, USA). The micropipette was then retracted 250 /textmum and an additional 1.5 l of virus solution was injected. To minimize leaking, the micropipette was left in place for 8 min after each injection. In total, the experimental group received a dose of 200 ng of recombinant TNF-α to right auditory cortex. After injection, the skin was sutured and the animals were returned to their home cages after regaining movement. For postoperative pain management, animals received subcutaneous injection of buprenorphine (0.05 mg/kg, SQ) and meloxicam (2 mg/kg, SQ).

Measuring GAD65 mRNA levels with RT-PCR

After behavioral testing, animals were euthanized with isoflurane. Brain tissue was collected from the right and left auditory cortices based on anatomical landmarks by an experienced experimenter. A coronal slice of approximately 1mm thickness (estimated stereotaxic coordinates: -2 mm to -3 mm bregma) was made using the dorsal-ventral extent of the hippocampus as landmarks. We then hemisected and isolated the auditory cortex at each side by making two orthogonal cuts to the cortical surface at 1 mm and 2 mm dorsal to the lingual gyrus. Subcortical structures were removed and two 1 mm cubes of cortical tissue, one from each side, were collected. These samples presumably included the primary auditory cortex and possibly other fields of the auditory cortex.

Reverse transcription polymerase chain reaction (RT-PCR) was conducted by an experimenter who was blind to the experimental conditions. Total RNA samples were prepared from the tissue with RNA Wiz (Ambion) according to the manufacturers instructions. The total RNA obtained (3/textmug) was reverse-transcribed using a first-strand cDNA synthesis kit (BD Biosciences, Palo Alto, CA). The PCR mixture (50 /textmul) contained 10 Taq buffer, 0.3 U Taq polymerase (Perkin-Elmer), 2.5 M of dNTPs, 5 pmol of each set of primers, and 50 ng of cDNA from the auditory cortex as template. GAD65-specific fragments were amplified with the following PCR primers: GAD65-F: 5-GCGCAGTTCTTGCTGGAAGTGGTAGACATA
3, GAD65-R: 5-AGGGTTCCAGGTGACTGAATTGGCCCTTTC-3. PCR reactions were performed under the following cycling conditions: an initial denaturation at 94 C for 5 min followed by 25-40 cycles of denaturation at 94C for 30 s, annealing at 63C for 30 s, and elongation at 72C for 1 min with a final elongation step at 72C for 10 min. A 10-/textmul sample of each PCR reaction was removed after 25 cycles, while the remaining mixture underwent 5 more cycles of amplification. The extent of amplification was chosen empirically to avoid saturation of the amplified bands. In addition, two samples were collected for optimal quantification of GAD65 expression levels. Each primer set yielded a PCR product of 870 bp in length for GAD65. The 18S rRNA gene was used as an internal standard (QuantumRNA, Ambion). To quantify PCR products, each sample was run in a 1.5% agarose gel and stained

with ethidium bromide. Band intensity was measured with an Alphaimager (Alpha Innotech Corp.) using the Alphaease (v3.3b) program.

Electrophysiological Recording Procedure

The primary auditory cortex (AI) in naïve and sound-exposed KO and WT mice was mapped as previously described (Kim and Bao, 2009; Yang et al., in press). Mice were anesthetized with ketamine (100 mg/kg, IP) and xylazine (10 mg/kg, IP), and placed on a homeothermic heating pad at 36.5 C (Harvard Apparatus) in a sound attenuation chamber. The head was secured with a custom head-holder that left the ears unobstructed. The right auditory cortex was exposed and kept under a layer of silicone oil to prevent desiccation. Neural responses were recorded using tungsten microelectrodes (FHC) at a depth of 380-420 /textmu m below the cortical surface, presumably from the thalamorecipient layer. Responses to 25-ms tone pips of 41 frequencies (4 to 75 kHz, 0.1 octave spacing) and eight sound pressure levels (10-80 dB, 10-dB steps) were recorded to reconstruct the frequency-intensity receptive field. A TDT coupler model electrostatic speaker was used to present all acoustic stimuli and each frequency x intensity combination was repeated 3 times. Both ears were stimulated in isolation to record contralateral and ipsilateral receptive fields at each recorded site.

Multi-unit activity was evenly sampled from the primary auditory cortex (AI), which could be identified by its tonotopic orientation—higher frequencies are represented more rostrally and slightly more dorsally (Guo et al., 2012)—and location relative to cranial anatomical landmarks—AI was found consistently underneath the caudal half of the temporal-parietal bone suture. The border of AI was defined by unresponsive sites or sites whose CFs were incongruent with the AI tontopic gradient. Because KOs tended to have incomplete representations of low and high frequencies (Yang et al., in press), we carefully searched for those representations near the rostral and caudal ends of AI in both WTs and KOs, while maintaining the same sampling density. After monaural NIHL, cortical responses to the contralateral ear became weaker, therefore we defined AI by the ipsilateral ear responses or the location relative to anatomical landmarks.

Data Analysis

The receptive fields and response properties were computed using custom-made programs. First, the peri-stimulus time histogram (PSTH) was generated from responses to all 1032 (43 frequencies x 8 intensities x 3 repetitions) tone pips, with 1-ms bin size. The mean firing rate was calculated for each bin and smoothed with a 5-point mean filter. The multiunit firing rate in the 50-ms window prior to stimulus onset was taken as the mean spontaneous firing rate. Peak latency was defined as the time to the peak PSTH response between 7 and 50 ms after the stimulus onset. The response window was defined as the period encompassing the PSTH peak, in which the mean firing rate in every bin was higher than baseline firing rate. The onset latency was defined at onset of the response window. The tone-evoked response

was measured as the maximum firing rate within the response window. Spikes that occurred within the response window were counted to reconstruct the receptive field.

The frequency-intensity receptive field (RF) was determined using a smoothing and thresholding algorithm. The response magnitude was plotted in the frequency-intensity space, and smoothed with a 3×3 mean filter (For examples, see Yang et al., in press). It was then thresholded at 28% of the maximum value of the smoothed response magnitude. The largest contiguous response area was determined to be the receptive field. The raw responses in the suprathreshold area was defined as the isolated receptive field. RF size was computed as the number of responsive frequency-intensity pairs in the isolated receptive field. The threshold of the neuron was the lowest sound level that elicited responses in the isolated receptive field, and the characteristic frequency (CF) was defined as the frequency that elicited responses at the threshold intensity. Manual ratings were carried out by an experienced rater blind to experimental condition. The maximum RF response was the maximum number of spikes activated by a single frequency-intensity combination. The mean RF response was the mean number of spikes for all frequency-dB combinations within the receptive field. Since each frequency-intensity combination was repeated 3 times, the average of those 3 responses was taken. The receptive field size was the number of frequency-intensity combinations within the receptive field. Receptive field and map properties were analyzed using a three-way ANOVA with factors of genotype (WT or KO), experience (naïve or NIHL), and stimulation side (left or right). The statistical significance of differences between pairs of treatment means was assessed using Tukeys HSD multiple comparisons test.

4.4 Results

NIHL causes tinnitus in WT but not TNF-α KO mice

TNF-α KO mice do not show salicylate-induced tinnitus

Salicylate has been shown to increase central TNF-α expression ([[citation]]). We examined whether TNF-α is required for salicylate-induced tinnitus using TNF-α KO mice. Systemic injection of ?? mg/kg salicylate resulted in robust behavioral manifestation of tinnitus 30 min later in wildtype mice (Figure 2; treatment $\times$ frequency 2-way ANOVA, treatment effect, $F_{1,88} = 24.28$, $p < 0.0001$; interaction, $F_{3,88} = 2.749$, $p = 0.048$). However, TNF-α KO mice did not show tinnitus after administration of the same dose of salicylate (Figure 2; treatment x frequency 2-way ANOVA, treatment effect, $F_{1,88} = 0.96$, $p = 0.33$; interaction, $F_{3,88} = 1.685$, $p = 0.18$).

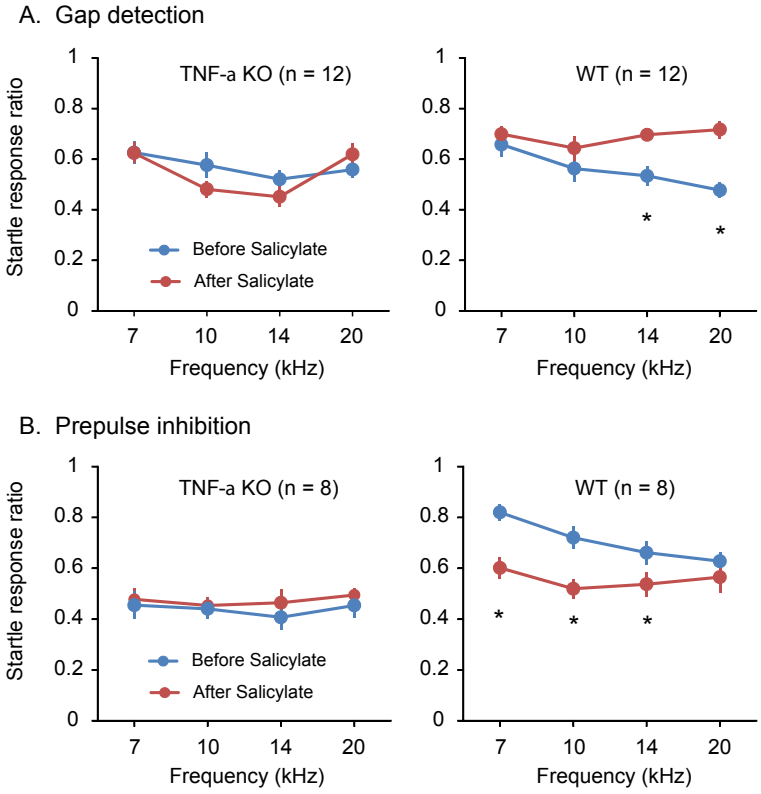

Figure 2.

Cortical infusion of recombinant TNF-α results in tinnitus

To test whether TNF-α is sufficient to cause tinnitus symptoms, we infused mouse recombinant TNF-α into the right hemisphere auditory cortex of normal-hearing WT and TNF-α KO mice. Control WT and KO mice were infused with carrier solution containing artificial cerebrospinal fluid and mouse albumin. Gap detection and PPI performance was examined in three daily sessions prior to the injection and only the third session was used as the baseline performance. Mice were tested again after 3 days of post-surgical recovery. Gap detection performance was analyzed with a 4-way ANOVA on genotype (WT vs. KO), treatment (before vs. after infusion), drug (TNF-α vs. albumin) and frequency of the background tone. There were main effects of treatment ($F_{1,152} = 8.619$, $p = 0.0038$) and drug ($F_{1,152} = 4.476$, $p = 0.032$). There was also treatment x drug interaction ($F_{1,152} = 5.730$, $p = 0.018$), indicating that TNF-α and albumin changed gap detection performance differently. However, the interaction was independent of genotype (treatment x drug x genotype interaction, $F_{1,152} = 0.007$, $p = 0.94$) suggesting that TNF-α infusion had similar effects on both WT and KO mice. Posthoc t-test indicates that TNF-α significantly impaired gap detection at 20 kHz (WT: t12 = 4.19, $p = 0.0013$; KO: t12 = 2.45, $p = 0.035$), but not at other frequencies.

A similar 4-way ANOVA on PPI failed to show significant treatment x drug interaction ($F_{1,152} = 0.391$, $p = 0.53$) indicating that TNF-α did not alter PPI performance (Figure 3).

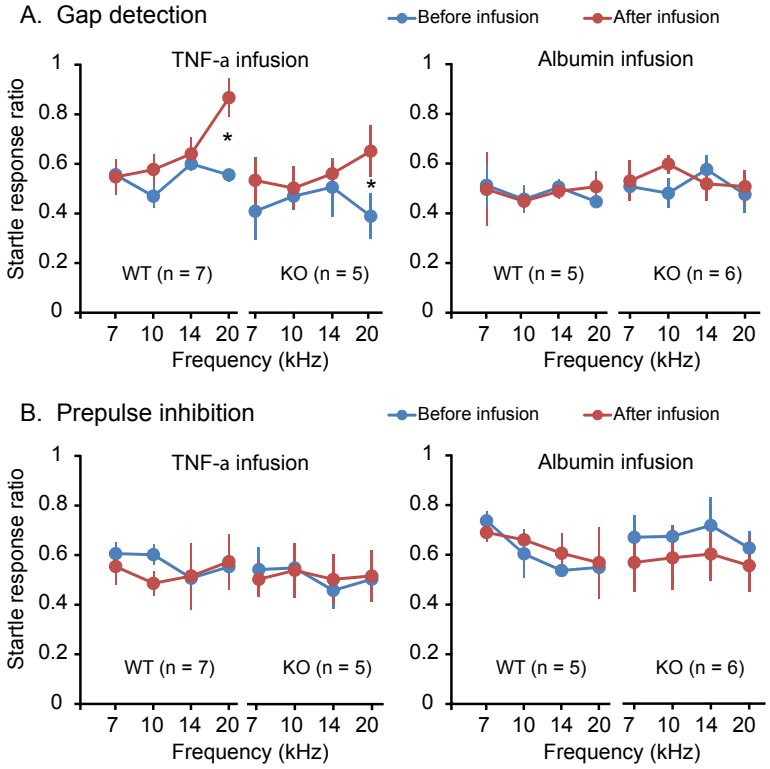

Figure 3. TNF-α is sufficient to cause tinnitus. (A) Auditory cortical infusion of mouse recombinant TNF-α results in behavioral signs of tinnitus both WT and TNF-α KO mice, as indicated by impaired gap detection performance. Infusion of mouse albumin did not result in tinnitus. (B) Prepulse inhibition was not altered by infusion of TNF-α or albumin. $^*p < 0.05$.

Hearing loss-induced downregulation of GAD65 expression was reduced in TNF-α KO mice

Plasticity of ipsilateral inputs following contralateral hearing lesion is impaired in TNF-α KO mice

To examine the electrophysiological changes in primary auditory cortex following unilateral NIHL, we independently stimulated the lesioned and intact ear while recording multi-unit activity from auditory cortex contralateral to the lesioned ear. Naïve WT and KO animals displayed strong, tonotopically-organized RFs in response to contralateral stimulation (Figure 4). As reported previously (Yang et al., 2013), evoked firing rates are lower in KO animals (WT-Left-naïve vs KO-Left-naïve, $p = 0.0190$, Tukeys HSD). Unilateral NIHL led to a drastic reduction in the proportion of units responsive to the lesioned ear in both genotypes,

however only in WT mice did NIHL result in a significant increase in the proportion of units responsive to the spared ear in ipsilateral cortex (Naïve vs NIHL, WT-Left: $p << 0.001$, KO-Left: $p = 0.0011$, WT-Right: $p = 0.012$, KO-Right: $p = 0.999$, Tukeys HSD, Figure 5A). The mean evoked firing rate and RF size showed similar patterns of changes following NIHL, i.e., decreases in both genotypes for contralateral stimulation, and increases only in WT animals for ipsilateral stimulation (Naïve vs NIHL, mean evoked firing rate: WT-Left: $p << 0.001$, KO-Left: $p = 0.166$, WT-Right: $p = 0.045$, KO-Right: $p = 1.00$, Figure 5B; RF size: WT-Left: $p << 0.001$, KO-Left: $p = 0.0170$, WT-Right: $p = 0.007$, KO-Right: $p = 0.999$, Tukeys HSD; Figure 5C). One exception was that in KO animals the decrease in mean firing rate for contralateral stimulation post-NIHL was a trend that did not reach significance.

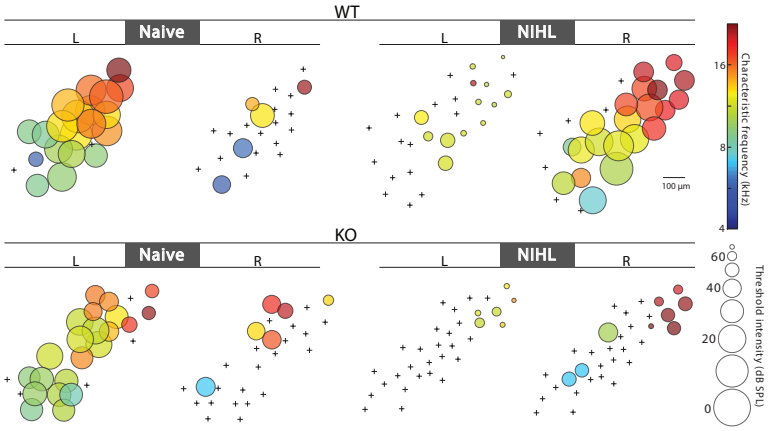

Figure 4. Example contralateral (L) and ipsilateral (R) maps for WT and KO in nave and NIHL animals. Each circle represents the multi-unit recording from one site, with characteristic frequency and threshold intensity represented by color and radius, respectively. Unresponsive sites are marked by a +. In nave WT and KO animals, contralateral maps in nave animals have low thresholds and few non-responsive sites, while ipsilateral maps have few responsive sites. Contralateral responses are nearly eliminated following NIHL in WT and KO, however only WT animals show strong augmentation of the ipsilateral map.

Bibliography

Abbott, S. D. et al. (1999). "Detection of glutamate decarboxylase isoforms in rat inferior colliculus following acoustic exposure". In: *Neuroscience* 93, pp. 1375–1381.

Browne, Cherylea J., John W. Morley, and Carl H. Parsons (2012). "Tracking the expression of excitatory and inhibitory neurotransmission-related proteins and neuroplasticity markers after noise induced hearing loss". In: *PLoS ONE* 7.

Davis, G W and I Bezprozvanny (2001). "Maintaining the stability of neural function: a homeostatic hypothesis." In: *Annual review of physiology* 63, pp. 847–869.

Fournier, Philippe and Sylvie H??bert (2013). "Gap detection deficits in humans with tinnitus as assessed with the acoustic startle paradigm: Does tinnitus fill in the gap?" In: *Hearing Research* 295, pp. 16–23.

Guo, W. et al. (2012). *Robustness of Cortical Topography across Fields, Laminae, Anesthetic States, and Neurophysiological Signal Types*.

Kaneko, Megumi et al. (2008). "Tumor Necrosis Factor-α Mediates One Component of Competitive, Experience-Dependent Plasticity in Developing Visual Cortex". In: *Neuron* 58, pp. 673–680.

Kim, Heesoo and Shaowen Bao (2009). "Selective increase in representations of sounds repeated at an ethological rate." In: *The Journal of neuroscience : the official journal of the Society for Neuroscience* 29, pp. 5163–5169.

Kotak, Vibhakar C et al. (2005). "Hearing loss raises excitability in the auditory cortex." In: *The Journal of neuroscience : the official journal of the Society for Neuroscience* 25, pp. 3908–3918.

Llano, Daniel a, Jeremy Turner, and Donald M. Caspary (2012). "Diminished cortical inhibition in an aging mouse model of chronic tinnitus." In: *The Journal of neuroscience : the official journal of the Society for Neuroscience* 32, pp. 16141–8.

Milbrandt, J. C. et al. (2000). "GAD levels and muscimol binding in rat inferior colliculus following acoustic trauma". In: *Hearing Research* 147, pp. 251–260.

Roberts, Larry E et al. (2010). "Ringing ears: the neuroscience of tinnitus." In: *The Journal of neuroscience : the official journal of the Society for Neuroscience* 30, pp. 14972–14979.

Steinmetz, Celine C and Gina G Turrigiano (2010). "Tumor necrosis factor-α signaling maintains the ability of cortical synapses to express synaptic scaling." In: *The Journal of neuroscience : the official journal of the Society for Neuroscience* 30, pp. 14685–14690.

Stellwagen, David and Robert C Malenka (2006). "Synaptic scaling mediated by glial TNF-alpha." In: *Nature* 440, pp. 1054–1059.

Stellwagen, David et al. (2005). "Differential regulation of AMPA receptor and GABA receptor trafficking by tumor necrosis factor-alpha." In: *The Journal of neuroscience : the official journal of the Society for Neuroscience* 25, pp. 3219–3228.

Turner, Jeremy G et al. (2006). "Gap detection deficits in rats with tinnitus: a potential novel screening tool." In: *Behavioral neuroscience* 120, pp. 188–195.

Turrigiano, Gina G. (1999). *Homeostatic plasticity in neuronal networks: The more things change, the more they stay the same.*

Wang, Hongning, Thomas J. Brozoski, and Donald M. Caspary (2011). *Inhibitory neurotransmission in animal models of tinnitus: Maladaptive plasticity.*

Yang, S., W. Su, and Shaowen Bao (2012). *Long-term, but not transient, threshold shifts alter the morphology and increase the excitability of cortical pyramidal neurons.*

Yang, Sungchil et al. (2011). "Homeostatic plasticity drives tinnitus perception in an animal model." In: *Proceedings of the National Academy of Sciences of the United States of America* 108, pp. 14974–14979.

Yang, Sungchil et al. (2013). "Impaired Development and Competitive Refinement of the Cortical Frequency Map in Tumor Necrosis Factor-α-Deficient Mice." In: *Cerebral cortex (New York, N.Y. : 1991).*

Bibliography

Abbott, S. D. et al. (1999). "Detection of glutamate decarboxylase isoforms in rat inferior colliculus following acoustic exposure". In: *Neuroscience* 93, pp. 1375–1381.

Browne, Cherylea J., John W. Morley, and Carl H. Parsons (2012). "Tracking the expression of excitatory and inhibitory neurotransmission-related proteins and neuroplasticity markers after noise induced hearing loss". In: *PLoS ONE* 7.

Davis, G W and I Bezprozvanny (2001). "Maintaining the stability of neural function: a homeostatic hypothesis." In: *Annual review of physiology* 63, pp. 847–869.

Fournier, Philippe and Sylvie H??bert (2013). "Gap detection deficits in humans with tinnitus as assessed with the acoustic startle paradigm: Does tinnitus fill in the gap?" In: *Hearing Research* 295, pp. 16–23.

Guo, W. et al. (2012). *Robustness of Cortical Topography across Fields, Laminae, Anesthetic States, and Neurophysiological Signal Types*.

Kaneko, Megumi et al. (2008). "Tumor Necrosis Factor-α Mediates One Component of Competitive, Experience-Dependent Plasticity in Developing Visual Cortex". In: *Neuron* 58, pp. 673–680.

Kim, Heesoo and Shaowen Bao (2009). "Selective increase in representations of sounds repeated at an ethological rate." In: *The Journal of neuroscience : the official journal of the Society for Neuroscience* 29, pp. 5163–5169.

Kotak, Vibhakar C et al. (2005). "Hearing loss raises excitability in the auditory cortex." In: *The Journal of neuroscience : the official journal of the Society for Neuroscience* 25, pp. 3908–3918.

Llano, Daniel a, Jeremy Turner, and Donald M. Caspary (2012). "Diminished cortical inhibition in an aging mouse model of chronic tinnitus." In: *The Journal of neuroscience : the official journal of the Society for Neuroscience* 32, pp. 16141–8.

Milbrandt, J. C. et al. (2000). "GAD levels and muscimol binding in rat inferior colliculus following acoustic trauma". In: *Hearing Research* 147, pp. 251–260.

Roberts, Larry E et al. (2010). "Ringing ears: the neuroscience of tinnitus." In: *The Journal of neuroscience : the official journal of the Society for Neuroscience* 30, pp. 14972–14979.

Steinmetz, Celine C and Gina G Turrigiano (2010). "Tumor necrosis factor-α signaling maintains the ability of cortical synapses to express synaptic scaling." In: *The Journal of neuroscience : the official journal of the Society for Neuroscience* 30, pp. 14685–14690.

Stellwagen, David and Robert C Malenka (2006). "Synaptic scaling mediated by glial TNF-alpha." In: *Nature* 440, pp. 1054–1059.

Stellwagen, David et al. (2005). "Differential regulation of AMPA receptor and GABA receptor trafficking by tumor necrosis factor-alpha." In: *The Journal of neuroscience : the official journal of the Society for Neuroscience* 25, pp. 3219–3228.

Turner, Jeremy G et al. (2006). "Gap detection deficits in rats with tinnitus: a potential novel screening tool." In: *Behavioral neuroscience* 120, pp. 188–195.

Turrigiano, Gina G. (1999). *Homeostatic plasticity in neuronal networks: The more things change, the more they stay the same.*

Wang, Hongning, Thomas J. Brozoski, and Donald M. Caspary (2011). *Inhibitory neurotransmission in animal models of tinnitus: Maladaptive plasticity.*

Yang, S., W. Su, and Shaowen Bao (2012). *Long-term, but not transient, threshold shifts alter the morphology and increase the excitability of cortical pyramidal neurons.*

Yang, Sungchil et al. (2011). "Homeostatic plasticity drives tinnitus perception in an animal model." In: *Proceedings of the National Academy of Sciences of the United States of America* 108, pp. 14974–14979.

Yang, Sungchil et al. (2013). "Impaired Development and Competitive Refinement of the Cortical Frequency Map in Tumor Necrosis Factor-α-Deficient Mice." In: *Cerebral cortex (New York, N.Y. : 1991).*